parasite infection. In fact, IL-18 is stored in bronchial and intestinal epithelium (43, 44), and it is quite possible that *S. venezuelensis* locally stimulates epithelial cells to produce IL-18.

Helmby and Grencis (45) have reported that daily injection of 0.2 μg of IL-18 into WT mice during infection with *Trichinella spiralis* decreased the mastocytosis as well as IL-13 secretion from mesenteric lymph node stimulated with *T. spiralis* antigen. Also, IL-18$^{-/-}$ mice infected with *T. spiralis* developed a high level of mastocytosis in the intestine during infection, correlating with the rapid expulsion of the parasites. These results suggest that IL-18 negatively regulates intestinal mastocytosis and Th2 cytokine production. In sharp contrast, our results presented here reveal that pretreatment of normal mice with IL-18 and IL-2 induces significant recruitment and activation of intestinal MMCs, resulting in extremely rapid expulsion of adult *S. venezuelensis* worms. Our findings clearly indicate that IL-18 positively regulates intestinal mastocytosis in the presence of IL-2 and that treatment with IL-18 plus IL-2 has provided host mice with type 2 innate immunity that protects against gastrointestinal nematode infection.

There are several possibilities that account for these discrepancies. Studies have contrasted the role of IL-4 in STAT6$^{-/-}$ mice infected with either *T. spiralis* or *Nippostrongylus brasiliensis*. *N. brasiliensis* infection of STAT 6$^{-/-}$ mice increase MMC and serum mMCP-1 levels, possibly through a primary Th2 response (33, 34). In contrast, MMC numbers and serum mMCP-1 responses were greatly decreased in STAT 6$^{-/-}$ mice infected with *T. spiralis*, and a reduced Th2 response resulted in lower IgG1 production (46). Therefore, type 2 cytokine responses are suppressed in STAT6$^{-/-}$ mice infected with *T. spiralis*, even though these responses are normal in STAT6$^{-/-}$ mice inoculated with *N. brasiliensis*. In other words, expulsion of *T. spiralis* is solely dependent on an STAT6-mediated signal that is required to stimulate the conditions that induce mast cells to degranulate optimally.

Helmby and Grencis reported that critical effects of IL-18 in *T. spiralis* infection are independent of IFN-γ and are mediated by the direct down-regulatory effect of IL-18 on IL-13 (45). It is important to point out that *N. brasiliensis* inoculation stimulates an almost pure type 2 cytokine response, whereas *T. spiralis* induces production of considerable IFN-γ in addition to IL-4. In this regard, adult *T. spiralis* live within various cells and induce considerably more IFN-γ production, probably through the induction of IL-12, than do *N. brasiliensis*, which live outside cells. Alternatively, *N. brasiliensis* may inhibit IL-12 production by DCs and macrophages. Therefore, it is possible that the work by Helmby and Grencis depicts a down-regulatory role of IL-18 on the Th2 response in the presence of IL-12 and its up-regulatory role on the Th1 response in the early phase of *T. spiralis* infections. In contrast to *T. spiralis* infection, *S. venezuelensis* infection resembles *N. brasiliensis* infection in its extracellular location in the host. It is possible that IL-2 is produced in the early phase of *S. venezuelensis* infection, which, along with endogenous IL-18, promotes MMC activation and accumulation in the intestinal mucosa independently of STAT6-mediated signal.

Here, we present a new paradigm of IL-18 activity in the host mucosal immune response against gastrointestinal nematode infections. IL-18, together with IL-12, plays an important role in the elimination of intracellular infections (3, 18), and, with IL-2, it can eradicate gastrointestinal nematode infections by induction of functional intestinal MMCs. Thus, IL-18 plays an important role in the host defense against both intracellular and extracellular pathogens, and the cytokine milieu of IL-18 determines its final effect on infected parasites. At present, we have not yet identified the cell source of IL-18 in mice inoculated with *S. venezuelensis*. Our present results indicate that *S. venezuelensis* expulsion might be induced by two types of intestinal MMC activation, IL-18–dependent (innate type 2) MMC activation and Th2 cell–dependent (acquired type 2) MMC activation. We also suggest a strong contribution of IL-3 and IL-9 in inducing mMCP-1 production from MMCs.

MATERIALS AND METHODS

Mice and reagents. Specific pathogen-free male C57BL/6 mice and Wistar rats were obtained from Charles River Breeding Laboratories. Mast cell-deficient WBB6F1-W/W^{v} mice (37) and littermate control WBB6F1$^{+/+}$ mice were purchased from SLC Japan. C57BL/6 RAG-2$^{-/-}$ mice were obtained from Taconic. Generation of C57BL/6 STAT6$^{-/-}$, IL-18$^{-/-}$, and IL-18Rα$^{-/-}$ mice has been detailed in our previous reports (47–49). All mice were bred under specific pathogen-free conditions at the animal facilities of Hyogo College of Medicine, Nishinomiya, Japan, and were used at 8 to 12 wk of age. All animal experiments were conducted according to the Guidelines for Animal Experiments at Hyogo College of Medicine. Recombinant human IL-2 was provided by Ajinomoto Co., Inc. Recombinant mouse IL-18 and IL-3/IL-9 were purchased from MBL International Corporation and from Genzyme. Anti-mouse IL-9 mAb (clone, D8402E8), biotinylated anti-mouse IL-9 mAb (clone, D9302C12), and anti-mouse IL-2 mAb (clone, S4B6, rat IgG2a) were purchased from BD Biosciences. Rabbit neutralizing anti-mouse-IL-18 IgG and control IgG antibodies were partially purified using Protein-A sepharose column in our laboratory. This anti–IL-18 antibody could completely neutralize 50 ng/ml of IL-18 at the concentration of 10 μg/ml in vitro. The administration of 200 μg of anti-IL-18 antibody just before LPS challenge completely inhibited LPS-induced liver injury in mice (11). Rat antibodies against mouse IL-4 (11b11) and IL-4Rα chain (M1) were purified in our laboratory. Intraperitoneal administration of a mixture of 10 mg of anti-IL-4 and 10 mg of IL-4Rα antibodies 1 d before anti-IgD challenge completely inhibited anti-IgD–induced IgE production in vivo (50).

Parasites. *S. venezuelensis* has been maintained in serial passage in male Wister rats in our laboratory. *S. venezuelensis* L3 were obtained from fecal culture by a filter paper method (36). Adult worms for intraduodenal implantation were prepared as follows. Wister rats were inoculated with 30,000 infective larvae, and the upper half of the small intestines were removed 7 to 10 d after infection. The intestine was then cut open longitudinally and washed with PBS followed by incubation at 37°C for 80 min. Worms that emerged from the intestine were washed with sterile PBS and adjusted to an appropriate density. Adult worms suspended in 500 μl of PBS were injected into the duodenum of recipient mice (1,500 worms/mouse) under anesthesia using a 1-ml syringe with a 22-gauge needle. Animals were inoculated s.c. with 5,000 *S. venezuelensis* L3 to initiate a complete infection. The degree of infection of individual mice was monitored by counting the number of eggs excreted daily (eggs/g feces).

In vivo treatment of mice. C57BL/6 normal, C57BL/6 STAT6$^{-/-}$, RAG-2$^{-/-}$, WBB6F1$^{+/+}$, or WBB6F1-W/W^{v} mice were injected i.p. daily with PBS alone or with various combinations of IL-18 (0.5–2 μg/d) and/or IL-2 (2×10^3–1×10^4 U/d) for 13 d. To deplete CD4$^+$ T cells, C57BL/6 mice were injected i.p. with monoclonal antibody to CD4 (clone, GK1.5; 0.5 mg/d; ATCC: TIB-207) or control antibody (rat IgG2b; 0.5 mg/d; BD Biosciences) 7 and 4 d before and 0, 3, and 7 d after IL-2 and/or IL-18 injection. For some experiments, C57BL/6 mice were injected daily with IL-3 (0.013–0.1 μg/d) and/or IL-9 (0.5 μg/d) for 13 d. These mice were killed on day 14 after cytokine treatments, and intestines, lungs, spleens, kidneys, and livers were removed for histological examination.

Intraduodenal adult worm implantation. To measure the invasion of adult *S. venezuelensis* into mouse intestinal mucosa, adult worms were implanted in the duodenum of recipient mice that had been treated with PBS or IL-2 and/or IL-18 for 13 d, and the mouse intestines were removed 16 h after implantation as described previously (36). Briefly, the intestine was cut open longitudinally and washed lightly to remove fecal matter and worms that were still in the lumen. Then the intestines were incubated at 37°C in PBS for 3 h. The number of worms that emerged from the intestines was counted. As we have reported previously, mucosal invasion of adult *S. venezuelensis* in naive host mice was completed within 4 h, and these implanted worms were rejected beyond 7 d after implantation in a mast cell–dependent mechanism (36). Based on these results, we recovered invading worms at 16 h after implantation.

ELISA. Mouse IL-9 was assayed by a specific sandwich ELISA with reference standard curves using known amounts of IL-9. To detect IL-9, we used anti-IL-9 mAb (D8402E8) and biotinylated anti-mouse IL-9 mAb (D9302C12; reference 22). The detection limit of this ELISA is 20 pg/ml. ELISA kits for IL-3, IL-4, and IL-13 (R&D Systems), and IL-18 (MBL International Corporation) were used. Levels of mMCP-1 in serum were measured with an mMCP-1 ELISA kit purchased from Moredun Scientific, Ltd.

Histological examination. For histological examination of MMC, tissue samples (8–10 cm) were removed from the pyloric ring. The intestine was opened longitudinally, flattened on a filter paper, and fixed in Carnoy's fluid and stained with Alcian blue, pH 0.3, and Safranin-O, as described previously (51). The number of mast cells in the epithelium and lamina propria mucosa was counted in 10 villous crypt units (VCU) according to the method described by Miller & Jarrett (52). Immunohistochemical staining for mMCP-1 on 6-μm-thick, paraffin wax–embedded, 10% formalin–fixed sections was performed as follows. The dew-axed sections were treated with 0.3% H_2O_2 in methanol for 30 min, then incubated with 10% normal rabbit serum in PBS for 1 h. The slides were incubated by sheep anti–mMCP-1 (Moredun Scientific, Ltd.) or normal sheep serum (Sigma-Aldrich) for 1 h, followed by incubation with peroxidase-conjugated rabbit anti-sheep IgG (Betty Laboratories, Inc.), and DAB reaction was performed.

We would like to thank Dr. W.E. Paul for his critical reading of this manuscript and C. Eguchi for her excellent experimental assistance.

This study is supported by a Grant-in-Aid for Scientific Research on Priority Areas and a Hitech Research Center grant from the Ministry of Education, Culture, Sports, Science and Technology of Japan.

The authors have no conflicting financial interests.

Submitted: 26 October 2004
Accepted: 6 July 2005

REFERENCES

1. Finkelman, F.D., D.T. Shea, J. Goldhill, C.A. Sullivan, S.C. Morris, K.B. Madden, W.C. Gause, and J.J. Urban. 1997. Cytokine regulation of host defense against parasitic gastrointestinal nematodes: lessons from studies with rodent models. *Annu. Rev. Immunol.* 15:505–533.
2. Grencis, R.K. 1997. Th2-mediated host protective immunity to intestinal nematode infections. *Philos. Trans. R. Soc. Lond. B Biol. Sci.* 352: 1377–1384.
3. Nakanishi, K., T. Yoshimoto, H. Tsutsui, and H. Okamura. K. 2001. Cytokine Therapeutic in Infectious Diseases. Lippincott Williams & Wilkins, Philadelphia. 343 pp.
4. Nakanishi, K., T. Yoshimoto, H. Tsutsui, and H. Okamura. 2001. Interleukin-18 regulates both Th1 and Th2 responses. *Annu. Rev. Immunol.* 19:423–474.
5. Reiner, S.L., and R.M. Locksley. 1995. The regulation of immunity to *Leishmania major*. *Annu. Rev. Immunol.* 13:151–177.
6. Sher, A., and R.L. Coffman. 1992. Regulation of immunity to parasites by T cells and T cell-derived cytokines. *Annu. Rev. Immunol.* 10: 385–409.
7. Edelson, B.T., and E.R. Unanue. 2000. Immunity to Listeria infection. *Curr. Opin. Immunol.* 12:425–431.
8. Seki, E., H. Tsutsui, N.M. Tsuji, N. Hayashi, K. Adachi, H. Nakano, S. Yumikura-Futatsugi, O. Takeuchi, K. Hoshino, S. Akira, et al. 2002. Critical roles of myeloid differentiation factor 88-dependent proinflammatory cytokine release in early phase clearance of *Listeria monocytogenes* in mice. *J. Immunol.* 169:3863–3868.
9. Fukao, T., S. Matsuda, and S. Koyasu. 2000. Synergistic effects of IL-4 and IL-18 on IL-12-dependent IFN-g production by dendritic cells. *J. Immunol.* 164:64–71.
10. Munder, M., M. Mallo, K. Eichmann, and M. Modolell. 1998. Murine macrophages secrete interferon γ upon combined stimulation with interleukin (IL)-12 and IL-18: a novel pathway of autocrine macrophage activation. *J. Exp. Med.* 187:2103–2108.
11. Okamura, H., H. Tsutsi, T. Komatsu, M. Yutsudo, A. Hakura, T. Tanimoto, K. Torigoe, T. Okura, Y. Nukada, K. Hattorial, et al. 1995. Cloning of a new cytokine that induces IFN-γ production by T cells. *Nature.* 378:88–91.
12. Robinson, D., K. Shibuya, A. Mui, F. Zonin, E. Murphy, T. Sana, S.B. Hartley, S. Menon, R. Kastelein, F. Bazan, and A. O'Garra. 1997. IGIF dose not drive Th1 development but synergizes with IL-12 for interferon-γ production and activates IRAK and NFκB. *Immunity.* 7:571–581.
13. Tsutsui, H., K. Nakanishi, K. Matsui, K. Higashino, H. Okamura, Y. Miyazawa, and K. Kaneda. 1996. IFN-γ-inducing factor up-regulates Fas ligand-mediated cytotoxic activity of murine natural killer cell clones. *J. Immunol.* 157:3967–3973.
14. Yoshimoto, T., H. Okamura, Y.-I. Tagawa, Y. Iwakura, and K. Nakanishi. 1997. Interleukin 18 together with interleukin 12 inhibits IgE production by induction of interferon-gamma production from activated B cells. *Proc. Natl. Acad. Sci. USA.* 94:3948–3953.
15. Yoshimoto, T., K. Takeda, T. Tanaka, K. Ohkusu, S. Kashiwamura, H. Okamura, S. Akira, and K. Nakanishi. 1998. IL-12 up-regulates IL-18 receptor expression on T cells, Th1 cells, and B cells: synergism with IL-18 for IFN-γ production. *J. Immunol.* 161:3400–3407.
16. Yoshimoto, T., N. Nagai, K. Ohkusu, H. Ueda, H. Okamura, and K. Nakanishi. 1998. LPS-stimulated SJL macrophages produce IL-12 and IL-18 that inhibit IgE production in vitro by induction of IFN-γ production from CD3^{int}IL-2Rβ$^+$ T cells. *J. Immunol.* 161:1483–1492.
17. Kawakami, K., Y. Kinjo, S. Yara, K. Uezu, Y. Koguchi, M. Tohyama, M. Azuma, K. Takeda, S. Akira, and A. Saito. 2001. Enhanced gamma interferon production through activation of Vα4(+) natural killer T cells by alpha-galactosylceramide in interleukin-18-deficient mice with systemic cryptococcosis. *Infect. Immun.* 69:6643–6650.
18. Wei, X.Q., B.P. Leung, W. Niedbala, D. Piedrafita, G.J. Feng, M. Sweet, L. Dobbie, A.J. Smith, and F.Y. Liew. 1999. Altered immune responses and susceptibility to *Leishmania major* and *Staphylococcus aureus* infection in IL-18-deficient mice. *J. Immunol.* 163:2821–2828.
19. Ohkusu, K., T. Yoshimoto, K. Takeda, T. Ogura, S. Kashiwamura, Y. Iwakura, S. Akira, H. Okamura, and K. Nakanishi. 2000. Potentiality of interleukin-18 as a useful reagent for treatment and prevention of *Leishmania major* infection. *Infect. Immun.* 68:2449–2456.
20. Hoshino, T., H. Yagita, J.R. Ortaldo, R.H. Wiltrout, and H.A. Young. 2000. In vivo administration of IL-18 can induce IgE production through Th2 cytokine induction and up-regulation of CD40 ligand (CD154) expression on CD4+ T cells. *Eur. J. Immunol.* 30:

1998–2006.
21. Yoshimoto, T., H. Mizutani, H. Tsutsui, T.N. Noben, K. Yamanaka, M. Tanaka, S. Izumi, H. Okamura, W.E. Paul, and K. Nakanishi. 2000. IL-18 induction of IgE: dependence on $CD4^+$ T cells, IL-4 and STAT6. *Nat. Immunol.* 1:132–137.
22. Yoshimoto, T., B. Min, T. Sugimoto, N. Hayashi, Y. Ishikawa, Y. Sasaki, H. Hata, K. Takeda, K. Okumura, K.L. Van, et al. 2003. Nonredundant roles for CD1d-restricted natural killer T cells and conventional $CD4^+$ T cells in the induction of immunoglobulin E antibodies in response to interleukin 18 treatment of mice. *J. Exp. Med.* 197:997–1005.
23. Yoshimoto, T., H. Tsutsui, K. Tominaga, K. Hoshino, H. Okamura, S. Akira, W.E. Paul, and K. Nakanishi. 1999. IL-18, although antiallergic when administered with IL-12, stimulates IL-4 and histamine release by basophils. *Proc. Natl. Acad. Sci. USA.* 96:13962–13966.
24. Yamanaka, K., M. Tanaka, H. Tsutsui, T.S. Kupper, K. Asahi, H. Okamura, K. Nakanishi, M. Suzuki, N. Kayagaki, R.A. Black, et al. 2000. Skin-specific caspase-1-transgenic mice show cutaneous apoptosis and pre-endotoxin shock condition with a high serum level of IL-18. *J. Immunol.* 165:997–1003.
25. Konishi, H., H. Tsutsui, T. Murakami, S. Futatuki-Yumikura, K. Yamanaka, M. Tanaka, Y. Iwakura, N. Suzuki, K. Takeda, S. Akira, et al. 2002. IL-18 contributes to the spontaneous development of atopic dermatitis-like inflammatory skin lesion independently of IgE/stat6 under specific pathogen-free conditions. *Proc. Natl. Acad. Sci. USA.* 99: 11340–11345.
26. Knight, P.A., S.H. Wright, C.E. Lawrence, Y.Y. Paterson, and H.R. Miller. 2000. Delayed expulsion of the nematode *Trichinella spiralis* in mice lacking the mucosal mast cell-specific granule chymase, mouse mast cell protease-1. *J. Exp. Med.* 192:1849–1856.
27. Scudamore, C.L., L. McMillan, E.M. Thornton, S.H. Wright, G.F. Newlands, and H.R. Miller. 1997. Mast cell heterogeneity in the gastrointestinal tract: variable expression of mouse mast cell protease-1 (mMCP-1) in intraepithelial mucosal mast cells in nematode-infected and normal BALB/c mice. *Am. J. Pathol.* 150:1661–1672.
28. Urban, J.J., L. Schopf, S.C. Morris, T. Orekhova, K.B. Madden, C.J. Betts, H.R. Gamble, C. Byrd, D. Donaldson, K. Else, and F.D. Finkelman. 2000. Stat6 signaling promotes protective immunity against *Trichinella spiralis* through a mast cell- and T cell-dependent mechanism. *J. Immunol.* 164:2046–2052.
29. Wastling, J.M., C.L. Scudamore, E.M. Thornton, G.F. Newl, and H.R. Miller. 1997. Constitutive expression of mouse mast cell protease-1 in normal BALB/c mice and its up-regulation during intestinal nematode infection. *Immunology.* 90:308–313.
30. Galli, S.J., and I. Hammel. 1994. Mast cell and basophil development. *Curr. Opin. Hematol.* 1:33–39.
31. Hultner, L., C. Druez, J. Moeller, C. Uyttenhove, E. Schmitt, E. Rude, P. Dormer, and S.J. Van. 1990. Mast cell growth-enhancing activity (MEA) is structurally related and functionally identical to the novel mouse T cell growth factor P40/TCGFIII (interleukin 9). *Eur. J. Immunol.* 20:1413–1416.
32. Madden, K.B., J.J. Urban, H.J. Ziltener, J.W. Schrader, F.D. Finkelman, and I.M. Katona. 1991. Antibodies to IL-3 and IL-4 suppress helminth-induced intestinal mastocytosis. *J. Immunol.* 147:1387–1391.
33. Urban, J.F., Jr., N. Noben-Trauth, D.D. Donaldson, K.B. Madden, S.C. Morris, M. Collins, and F.D. Finkelman. 1998. IL-13, IL-4Rα, and Stat6 are required for the expulsion of the gastrointestinal nematode parasite *Nippostrongylus brasiliensis*. *Immunity.* 8:255–264.
34. Finkelman, F.D., S.C. Morris, T. Orekhova, M. Mori, D. Donaldson, S.L. Reiner, N.L. Reilly, L. Schopf, and J.F. Urban Jr. 2000. Stat6 regulation of in vivo IL-4 responses. *J. Immunol.* 164:2303–2310.
35. Lantz, C.S., J. Boesiger, C.H. Song, N. Mach, T. Kobayashi, R.C. Mulligan, Y. Nawa, G. Dranoff, and S.J. Galli. 1998. Role for interleukin-3 in mast-cell and basophil development and in immunity to parasites. *Nature.* 392:90–93.
36. Maruyama, H., Y. Yabu, A. Yoshida, Y. Nawa, and N. Ohta. 2000. A role of mast cell glycosaminoglycans for the immunological expulsion of intestinal nematode, *Strongyloides venezuelensis*. *J. Immunol.* 164: 3749–3754.
37. Kitamura, Y., S. Go, and K. Hatanaka. 1978. Decrease of mast cells in W/W^v mice and their increase by bone marrow transplantation. *Blood.* 52:447–452.
38. Huizinga, J.D., K. Ambrous, and T. Der-Silaphet. 1998. Co-operation between neural and myogenic mechanisms in the control of distension-induced peristalsis in the mouse small intestine. *J. Physiol.* 506:843–856.
39. Puddington, L., S. Olson, and L. Lefrancois. 1994. Interactions between stem cell factor and c-Kit are required for intestinal immune system homeostasis. *Immunity.* 9:733–739.
40. Miller, H.R., S.H. Wright, P.A. Knight, and E.M. Thornton. 1999. A novel function for transforming growth factor-β1: upregulation of the expression and the IgE-independent extracellular release of a mucosal mast cell granule-specific beta-chymase, mouse mast cell protease-1. *Blood.* 93:3473–3486.
41. Voehringer, D., K. Shinkai, and R.M. Locksley. 2004. Type 2 immunity reflects orchestrated recruitment of cells committed to IL-4 production. *Immunity.* 20:267–277.
42. Min, B., M. Prout, J. Hu-Li, J. Zhu, D. Jankovic, E.S. Morgan, J.F. Urban Jr., A.M. Dvorak, F.D. Finkelman, G. LeGros, and W.E. Paul. 2004. Basophils produce IL-4 and accumulate in tissues after infection with a Th2-inducing parasite. *J. Exp. Med.* 200:507–517.
43. Cameron, L.A., R.A. Taha, A. Tsicopoulos, M. Kurimoto, R. Olivenstein, B. Wallaert, E.M. Minshall, and Q.A. Hamid. 1999. Airway epithelium expresses interleukin-18. *Eur. Respir. J.* 14:553–559.
44. Pizarro, T.T., M.H. Michie, M. Bentz, J. Woraratanadharm, M.J. Smith, E. Foley, C.A. Moskaluk, S.J. Bickston, and F. Cominelli. 1999. IL-18, a novel immunoregulatory cytokine, is up-regulated in Crohn's disease: expression and localization in intestinal mucosal cells. *J. Immunol.* 162:6829–6835.
45. Helmby, H.R., and K. Grencis. 2002. IL-18 regulates intestinal mastocytosis and Th2 cytokine production independently of IFN-γ during *Trichinella spiralis* infection. *J. Immunol.* 169:2553–2560.
46. Urban, J.F., Jr., L. Schopf, S.C. Morris, T. Orekhova, K.B. Madden, C.J. Betts, H.R. Gamble, C. Byrd, D. Donaldson, K. Else, and F.D. Finkelman. 2000. Stat6 signaling promotes protective immunity against *Trichinella spiralis* through a mast cell- and T cell-dependent mechanism. *J. Immunol.* 164:2046–2052.
47. Hoshino, K., H. Tsutsui, T. Kawai, K. Takeda, K. Nakanishi, Y. Takeda, and S. Akira. 1999. Cutting edge: generation of IL-18 receptor-deficient mice: evidence for IL-1 receptor-related protein as an essential IL-18 binding receptor. *J. Immunol.* 162:5041–5044.
48. Takeda, K., T. Tanaka, W. Shi, M. Matsumoto, M. Minami, S. Kashiwamura, K. Nakanishi, N. Yoshida, T. Kishimoto, and S. Akira. 1996. Essential role of Stat6 in IL-4 signalling. *Nature.* 380:627–630.
49. Takeda, K., H. Tsutsui, T. Yoshimoto, O. Adachi, N. Yoshida, T. Kishimoto, H. Okamura, K. Nakanishi, and S. Akira. 1998. Defective NK cell activity and Th1 response in IL-18-deficient mice. *Immunity.* 8:383–390.
50. Finkelman, F.D., J.F. Urban Jr., M.P. Beckmann, K.A. Schooley, J.M. Holmes, and I.M. Katona. 1991. Regulation of murine in vivo IgG and IgE responses by a monoclonal anti-IL-4 receptor antibody. *Int. Immunol.* 3:599–607.
51. Tegoshi, T., M. Okada, M. Nishida, and N. Arizono. 1997. Early increase of gut intraepithelial mast cell precursors following *Strongyloides venezuelensis* infection in mice. *Parasitology.* 114:181–187.
52. Miller, H.R., and W.F. Jarrett. 1971. Immune reactions in mucous membranes. I. Intestinal mast cell response during helminth expulsion in the rat. *Immunology.* 20:277–288.

Ann Hematol (2005) 84: 423–428
DOI 10.1007/s00277-005-1019-3

ORIGINAL ARTICLE

Nobuko Yamaguchi · Yoshihiro Fujimori · Yuka Fujibayashi · Ikuyo Kasumoto · Haruki Okamura · Kenji Nakanishi · Hiroshi Hara

Interferon-gamma production by human cord blood monocyte-derived dendritic cells

Received: 4 June 2004 / Accepted: 29 October 2004 / Published online: 6 April 2005

Abstract Interferon (IFN)-γ is produced by T cells and natural killer cells and activates monocytes and dendritic cells (DCs). Recently, IFN-γ has been shown to be produced by mouse DCs following stimulation with interleukin (IL)-12, which is markedly augmented by the addition of IL-18. We here analyzed whether human DCs secrete IFN-γ in response to IL-12 and/or IL-18. Human immature DCs, generated from cord blood $CD14^+$ monocytes by treating with granulocyte–macrophage colony-stimulating factor and IL-4, were incubated with IL-12 and/or IL-18 and assayed for IFN-γ production. IL-12, but not IL-18, weakly induced IFN-γ production, while IL-12 together with IL-18 induced high levels of IFN-γ production. Similar results were obtained with mature DCs, although levels of IFN-γ production were less than those in immature DCs. Also with mature and immature DCs, IL-12 upregulated the expression of IL-18 receptor α (Rα), and costimulation with IL-12 and IL-18 upregulated CD40 expression. Anti-IL-18Rα antibody abrogated both the IFN-γ induction and the CD40 upregulation by IL-12 plus IL-18. These findings suggest that IL-12 upregulates IL-18Rα expression on human DCs and acts synergistically with IL-18 to induce high levels of IFN-γ, which subsequently enhances CD40 expression on DCs in an autocrine manner.

Keywords Interferon-γ · Dendritic cells · Human · IL-18

N. Yamaguchi · Y. Fujibayashi · I. Kasumoto · H. Hara
Division of Hematology and Oncology,
Department of Medicine,
Hyogo College of Medicine,
1-1 Mukogawa-cho,
Nishinomiya, Hyogo, 663-8501, Japan

Y. Fujimori (✉)
Laboratory of Cell Transplantation,
Institute for Advanced Medical Sciences,
Hyogo College of Medicine,
1-1 Mukogawa-cho,
Nishinomiya, Hyogo, 663-8501, Japan
e-mail: fuji-y@hyo-med.ac.jp
Tel.: +81-798-456599
Fax: +81-798-456599

H. Okamura
Laboratory of Host Defences,
Institute for Advanced Medical Sciences,
Hyogo College of Medicine,
1-1 Mukogawa-cho,
Nishinomiya, Hyogo, 663-8501, Japan

K. Nakanishi
Department of Immunology and Medical Zoology,
Hyogo College of Medicine,
1-1 Mukogawa-cho,
Nishinomiya, Hyogo, 663-8501, Japan

Introduction

Dendritic cells (DCs) are professional antigen-presenting cells that have an extraordinary capacity to stimulate T cells and initiate primary immune responses [1]. DCs are characterized by a high capacity for antigen capture and processing, migration to lymphoid organs, and expression of costimulatory molecules, such as CD40. Cytokine secretion by DCs initiates and enhances both innate and acquired immunity [1].

Some microbial infections rapidly induce interleukin (IL)-12 production in DCs without T-cell interaction [19]. Another pathway to IL-12 production is dependent on T cells [3, 11]. Upon either antigen uptake or microbial infection, DCs display both elevated levels of CD40 expression and increased ability to produce IL-12 in response to CD40 ligand (CD40L) on T cells [3, 11]. The secreted IL-12 subsequently induces interferon (IFN)-γ production by natural killer (NK) cells and directs T-helper 1 (Th1) development [13]. IFN-γ acts on DCs to augment IL-12 secretion. Thus, IL-12 and IFN-γ comprise a positive feedback system and IFN-γ plays a major role in the clearance of intracellular pathogens [6].

IL-18, originally designated as IFN-γ-inducing factor, strongly augments IFN-γ production by T cells [16, 21]. High levels of IL-18 receptor α (Rα) expression correlate with the ability of IL-18 to induce as well as act synergistically with IL-12 for IFN-γ production [22]. The synergistic effect of IL-12 and IL-18 occurs in the absence of

T-cell receptor (TCR) ligation and may represent an alternative pathway for production of IFN-γ during an inflammatory response [16].

Although the production of IFN-γ was thought to be restricted to lymphoid cells, such as T and NK cells, it is now known to be produced by antigen-presenting cells (APCs) such as macrophages [5, 7, 8, 14, 18] and DCs [8, 9, 15, 20]. Most of the previous studies of relationships between IFN-γ and APCs were done with mouse cells and there is only one report on IFN-γ in human macrophages [7]. We investigated whether human cord blood-derived DCs secrete IFN-γ since NK cells and CD45RA(+) T cells in cord blood produce IFN-γ at levels comparable to those observed with adult blood counterparts stimulated by IL-12 plus IL-18 [17]. Here, we report that human cord blood-derived DCs secrete IFN-γ after costimulation with IL-12 and IL-18, which in turn upregulates CD40 expression in an autocrine manner.

Materials and methods

Cell preparation

Umbilical cord blood (CB) was obtained from normal full-term deliveries with the consent of the mother. Mononuclear cells (MCs) were separated by Ficoll–Paque density gradient centrifugation. T, NK, and B cells were depleted from MCs with fluorescein isothiocyanate (FITC)-conjugated CD3, CD19, CD20, CD56, and TCR αβ monoclonal antibodies (Abs) (Immunotech, Marseilles, France) and anti-FITC immunomagnetic beads using the automated magnetic cell sorter (autoMACS) system (Miltenyi Biotec, Auburn, Calif., USA). $CD14^+$ monocytes were then positively selected from the remaining MCs using CD14 immunomagnetic beads and autoMACS.

Induction of DCs

Human immature dendritic cells (IMDCs) were induced by culturing cord blood $CD14^+$ monocytes in RPMI-1640 medium (Sigma Chemical Co., St. Louis, Mo., USA) containing 10% fetal calf serum (Gibco BRL, Grand Island, N. Y., USA), 50 ng/ml granulocyte–macrophage colony-stimulating factor (GM-CSF) (Pepro Tech, London, UK), and 10 ng/ml IL-4 (Pepro Tech, London, UK) for 7 days. Mature DCs (MDCs) were induced by culturing IMDCs for an additional 2 days in the presence of IL-4, GM-CSF, and 10 ng/ml tumor necrosis factor (TNF)-α (Pepro Tech, London, UK).

IFN-γ assay

IMDCs or MDCs at 2×10^6/ml were incubated in RPMI-1640 medium in the presence of 100 ng/ml IL-12 (Pepro Tech, London, UK) and/or 100 ng/ml IL-18 (Hayashibara Biochemical Laboratories, Inc., Okayama, Japan) for 5 days in 96-well flat-bottom tissue culture plates. Time course experiments showed that 5 days of incubation was sufficient for IFN-γ induction. IFN-γ was assayed in triplicate by a commercially available enzyme-linked immunosorbent assay (ELISA) kit (Genzyme TECHNE, Boston, Mass., USA). In some experiments, 1 μg/ml of IL-18 receptor antibody (#117-10C) (Hayashibara Biochemical Laboratories, Inc., Okayama, Japan), which can block the biological activity of IL-18 [12], was added to the cultures. As control, isotype-matched control Ab (mouse IgM) was added to the cultures.

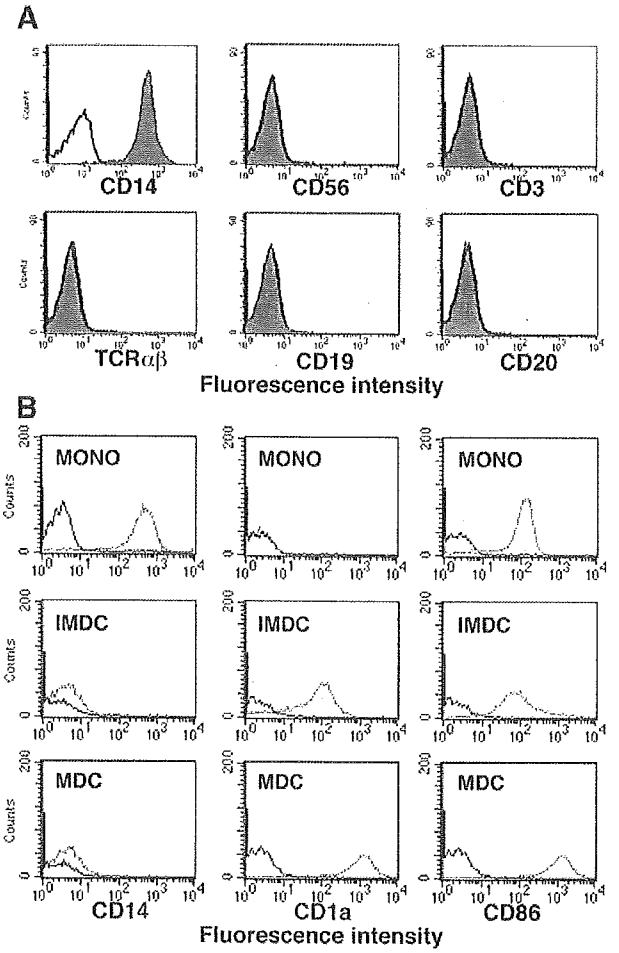

Fig. 1 Surface marker analysis of $CD14^+$ monocytes (*MONO*), immature dendritic cells (*IMDC*), and mature DCs (*MDC*). **a** Surface marker analysis of $CD14^+$ MACS-sorted cells. Cord blood mononuclear cells were first depleted CD3-, CD19-, CD20-, CD56- and TCR αβ-positive cells and then CD14-positive cells were selected as described in "Materials and methods." They were analyzed for the expression of antigens (*dark area*) by flow cytometry. *Open areas* show isotype-matched control. Data are representative of five independent experiments. **b** Surface marker analysis of $CD14^+$ monocytes (*MONO*), immature dendritic cells (*IMDC*) and mature DCs (*MDC*). IMDCs were induced by culturing $CD14^+$ monocytes in the presence of IL-4 and GM-CSF for 7 days. MDCs were induced by an additional incubation in the presence of IL-4, GM-CSF, and TNF-α for 2 days. They were analyzed for the expression of antigens (*dark area*) by flow cytometry. *Open areas* show isotype-matched control. Data are representative of five independent experiments.

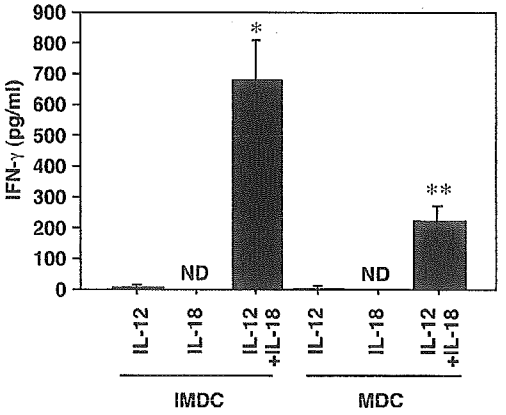

Fig. 2 IFN-γ production by DCs in the presence of IL-12 and/or IL-18. IMDCs and MDCs were cultured in the presence of IL-12 and/or IL-18 for 5 days and analyzed for IFN-γ in the medium by ELISA. Data are representative of five independent experiments and show mean±SEM of triplicate samples in each experimental group. *p<0.001, **p<0.01 in comparison with IL-12 alone. *ND* not detectable.

Flow cytometric analysis

Cells were stained with FITC- or phycoerythrin (PE)-conjugated Abs at 4°C for 30 min and immunofluorescence was analyzed using an EPICS XL flow cytometer (Coulter, Miami, Fla., USA). The specific Abs were PE-conjugated anti-IL-18Rα (R&D Systems, Minneapolis, Minn., USA) and FITC-conjugated anti-CD14, CD1a, CD83, CD86, CD40, CD3, CD19, CD20, CD56, and TCR αβ (Immunotech, Marseilles, France). The appropriate isotype-matched control Abs were used in all experiments. Relative mean fluorescence intensity (MFI) was calculated by dividing experimental MFI by control MFI. The cutoff value of relative MFI was 1.2.

Statistical analysis

Data are presented as mean±standard error of means (SEM). The nonparametric Mann–Whitney U test was used; p values <0.05 were considered to be significant.

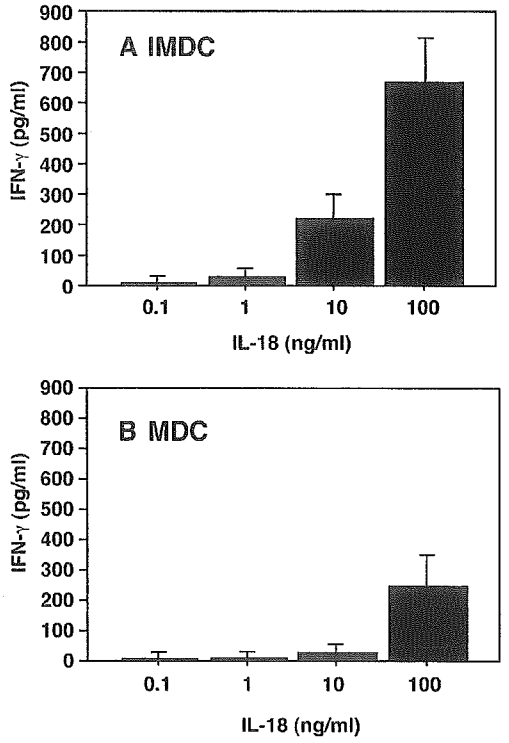

Fig. 3 Dose-dependent effect of IL-18 on IFN-γ production by DCs. IMDCs and MDCs were cultured in the presence of 100 ng/ml of IL-12 and various doses of IL-18 for 5 days and analyzed for IFN-γ in the medium by ELISA. Data are representative of five independent experiments and show mean±SEM of triplicate samples in each experimental group.

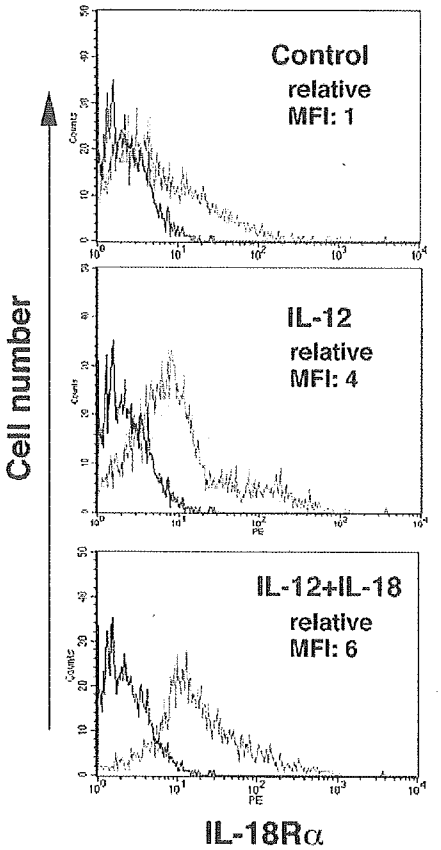

Fig. 4 Effects of IL-12 and IL-18 on the expression of IL-18Rα on DCs. IMDCs were cultured in the presence of IL-12 and/or IL-18 for 5 days and analyzed for IL-18Rα expression by flow cytometry. *Open areas* show isotype-matched control. Data are representative of five independent experiments. Relative mean fluorescence intensity (MFI)=experimental MFI/control MFI.

Results

Characterization of DCs induced by cord blood monocytes

More than 95% of the $CD14^+$ MACS-sorted cells expressed CD14, and they were undetectable for CD56 , CD3, TCR $\alpha\beta$, CD19, and CD20 (Fig. 1a). These $CD14^+$ monocytes (MONO) were cultured to induce DCs. The expression of DC-related surface markers is shown in Fig. 1b. Both IMDCs and MDCs became negative for CD14, but positive for CD1a. Expression of CD1a and CD86 was higher in MDCs than in IMDCs.

IFN-γ production by human DCs

We stimulated IMDCs and MDCs with IL-12 and IL-18, either alone or in combination, for IFN-γ production (Fig. 2). The stimulation of IMDCs with IL-12 alone, but not IL-18, resulted in the production of a small amount of IFN-γ. In contrast, IL-12 in combination with IL-18 induced a large amount of IFN-γ ($p<0.001$ in comparison with IL-12 alone). MDCs also showed significant IFN-γ production in response to IL-12 plus IL-18 ($p<0.01$ in comparison with IL-12 alone). However, levels of IFN-γ production in MDC were less than those in IMDCs (Fig. 2). In the presence of IL-12 held fixed at 100 ng/ml, the IFN-γ production in IMDCs increased with the addition of IL-18 in a dose-dependent manner (Fig. 3a). A similar dose–response effect was observed with MDCs, although levels of IL-18 production were lower than those in IMDCs (Fig. 3b).

Expression of IL-18Rα in human DCs

We next examined the expression of IL-18Rα in human DCs (Fig. 4). Stimulation of IMDCs with IL-12 alone resulted in upregulation of IL-18Rα expression on their surface. The combination of IL-12 and IL-18 further upregulated IL-18Rα expression in IMDCs (Fig. 4) and in MDCs (data not shown).

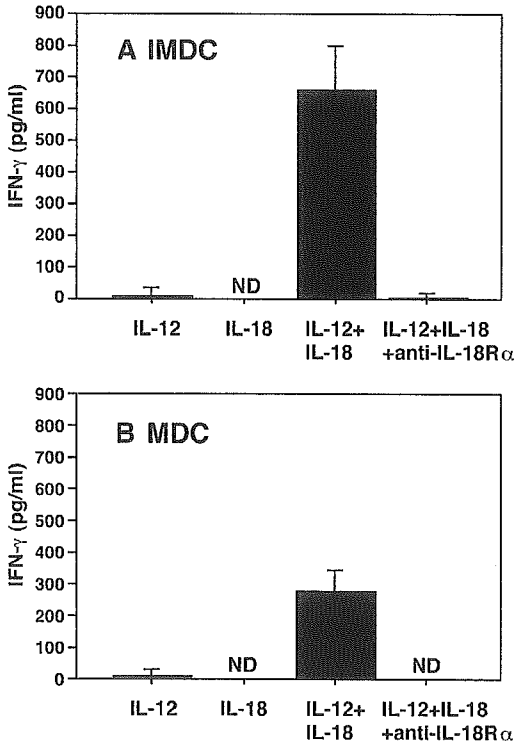

Fig. 5 Anti-IL-18Rα treatment abrogates IFN-γ production by DCs. IMDCs or MDCs were incubated with IL-12 and IL-18 in the presence of anti-IL-18Rα antibody or control mouse IgM antibody for 5 days and analyzed for IFN-γ in the medium by ELISA. Data are representative of five independent experiments and show mean± SEM of triplicate samples in each experimental group. *ND* not detectable.

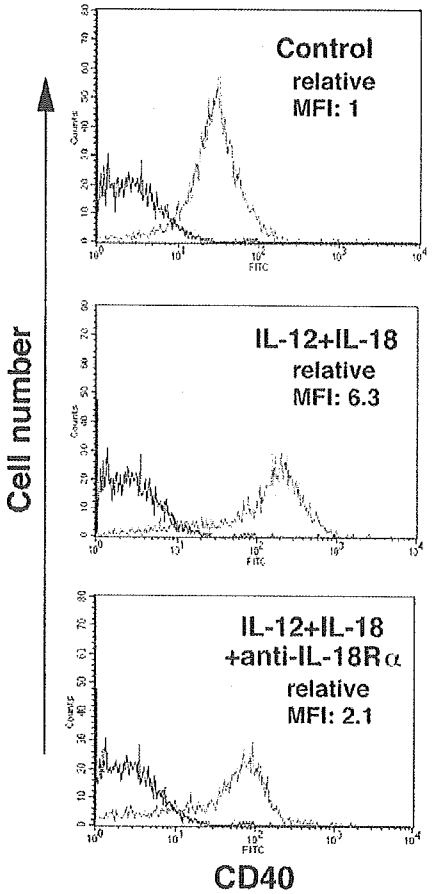

Fig. 6 Upregulation of CD40 on DCs by IL-12 plus IL-18. IMDCs were incubated with IL-12 and IL-18 in the presence of anti-IL-18Rα antibody or control mouse IgM antibody for 5 days and analyzed for CD40 expression by flow cytometry. *Open areas* show isotype-matched control. Data are representative of five independent experiments. Relative mean fluorescence intensity (MFI)=experimental MFI/control MFI.

Effect of anti-IL-18Rα antibody on IFN-γ production

We examined the effect of antibody to IL-18Rα on IFN-γ production in human DCs. As shown in Fig. 5, the addition of IL-18Rα antibody suppressed the production of IFN-γ in the presence of IL-12 and IL-18 in both IMDCs and MDCs. These results suggest that the IL-18 ligand and receptor system is critical to the production of IFN-γ in human DCs.

Upregulation of CD40 in human DCs

IMDCs used in this study expressed CD40 on their surface (Fig. 6, top panel). The CD40 level increased following treatment with IL-12 and IL-18 (Fig. 6, middle panel). The addition of IL-18Rα antibody suppressed the IL-12/IL-18-mediated upregulation of CD40 (Fig. 6, bottom panel), as in the case of IFN-γ production (Fig. 5). Similar results were obtained with MDCs (data not shown). Since IFN-γ upregulates CD40 expression, these results suggest that IFN-γ secreted by DCs following treatment with IL-12 and IL-18 enhances CD40 expression in an autocrine manner.

Discussion

Synergism between IL-12 and IL-18 in the induction of IFN-γ has been shown in human and murine T cells [21, 22] and NK cells [10, 23]. These cytokines also cooperatively induce IFN-γ secretion from murine B cells, macrophages, and DCs [5, 8, 9, 14, 15, 18, 20, 22]. In the present study, we examined whether human cord blood-derived DCs can secrete IFN-γ in response to the treatment with IL-12 and IL-18.

IL-12 alone induced IFN-γ from DCs at low levels, while IL-18 alone did not (Fig. 2). A combination of IL-12 and IL-18 induced IFN-γ at much higher levels than IL-12 alone, consistent with the reports with T and NK cells [10, 21]. IL-12 upregulated the expression of IL-18Rα on DCs (Fig. 4). Treatment of DCs with anti-IL-18Rα antibody abrogated the production of IFN-γ (Fig. 5). DCs stimulated by IL-12 and IL-18 upregulated CD40 expression on their surface, which was also downregulated by the treatment of anti-IL-18Rα antibody (Fig. 6). These findings suggest that IL-12 renders human DCs responsive to IL-18 to produce IFN-γ, which in turn activates DCs in an autocrine manner.

It has been known that DCs produce IL-12 upon phagocytosis of antigens during microbial infection [19] and that secreted IL-12 subsequently acts on NK cells and $CD4^+$ T cells to induce IFN-γ, which in turn activates DCs to increase their presentation of antigen [13]. Thus, the production of IFN-γ has been thought to be restricted to T and lymphoid cells. Our study using human cells and others using mouse cells [8, 9, 20] support the notion that DCs produce IL-12 and IFN-γ once they have been triggered by microbial infection. In addition to IL-12, IL-18 is also likely to be involved in enhancing IFN-γ production in DCs, as DCs are important producers of both IL-12 and IL-18 [16]. IFN-γ secreted may facilitate autocrine activation of DCs and activate macrophages to boost the ability to kill pathogens, thus augmenting innate immune responses. Compared to the fact that T cell-derived IFN-γ usually appears 2–4 days after infection [20], production of IFN-γ by DCs would occur early in infection, prior to specific recognition by T cells. IFN-γ produced by DCs at the time of antigen presentation would facilitate early polarization of Th1 response, since it is possible that a higher local concentration at sites of antigen presentation could amplify the effects of even a minimal amount of IFN-γ. Thus, the production of IFN-γ by DCs would act not only to enhance innate immunity but also to establish a link between innate immunity and adaptive immune responses.

Cord blood DCs have been reported to be functionally immature compared with adult DCs [2, 4]. However, cord blood NK cells and CD45RA(+) T cells produce IFN-γ at levels comparable to those observed with adult counterparts treated with IL-12 plus IL-18 [17]. The present study showed that cord blood-derived DCs were able to produce IFN-γ after stimulation with the combination of IL-12 and IL-18. Thus, our findings point to a novel understanding of the interaction between human DCs and T cells through early production of IFN-γ by DCs.

Acknowledgments This study was supported by a research grant for the Hitech Research Program from the Ministry of Education, Science, Sports and Culture of Japan, a grant from the Research on Human Genome, Tissue Engineering Food Biotechnology of the Ministry of Health and Welfare of Japan, and a Research Grant from Hyogo College of Medicine.

References

1. Banchereau J, Steinman RM (1998) Dendritic cells and the control of immunity. Nature 392:245–252
2. Borras FE, Matthews NC, Lowdell MW, Navarrete CV (2001) Identification of both myeloid CD11c+ and lymphoid CD11c– dendritic cell subsets in cord blood. Br J Haematol 113:925–931
3. Cella M, Scheidegger D, Palmer-Lehmann K, Lane P, Lanzavecchia A, Alber G (1996) Ligation of CD40 on dendritic cells triggers production of high levels of interleukin-12 and enhances T cell stimulatory capacity: T–T help via APC activation. J Exp Med 184:747–752
4. De Wit D, Tonon S, Olislagers V, Goriely S, Boutriaux M, Goldman M, Willems F (2003) Impaired responses to toll-like receptor 4 and toll-like receptor 3 ligands in human cord blood. J Autoimmun 21:277–281
5. Di Marzio P, Puddu P, Conti L, Belardelli F, Gessani S (1994) Interferon gamma upregulates its own gene expression in mouse peritoneal macrophages. J Exp Med 179:1731–1736
6. Dorman SE, Holland SM (2000) Interferon-gamma and interleukin-12 pathway defects and human disease. Cytokine Growth Factor Rev 11:321–333
7. Fenton MJ, Vermeulen MW, Kim S, Burdick M, Strieter RM, Kornfeld H (1997) Induction of gamma interferon production in human alveolar macrophages by Mycobacterium tuberculosis. Infect Immun 65:5149–5156
8. Frucht DM, Fukao T, Bogdan C, Schindler H, O'Shea JJ, Koyasu S (2001) IFN-gamma production by antigen-presenting cells: mechanisms emerge. Trends Immunol 22:556–560

9. Fukao T, Matsuda S, Koyasu S (2000) Synergistic effects of IL-4 and IL-18 on IL-12-dependent IFN-gamma production by dendritic cells. J Immunol 164:64–71
10. Hyodo Y, Matsui K, Hayashi N, Tsutsui H, Kashiwamura S, Yamauchi H, Hiroishi K, Takeda K, Tagawa Y, Iwakura Y, Kayagaki N, Kurimoto M, Okamura H, Hada T, Yagita H, Akira S, Nakanishi K, Higashino K (1999) IL-18 up-regulates perforin-mediated NK activity without increasing perforin messenger RNA expression by binding to constitutively expressed IL-18 receptor. J Immunol 162:1662–1668
11. Koch F, Stanzl U, Jennewein P, Janke K, Heufler C, Kampgen E, Romani N, Schuler G (1996) High level IL-12 production by murine dendritic cells: upregulation via MHC class II and CD40 molecules and downregulation by IL-4 and IL-10. J Exp Med 184:741–746
12. Kunikata T, Torigoe K, Ushio S, Okura T, Ushio C, Yamauchi H, Ikeda M, Ikegami H, Kurimoto M (1998) Constitutive and induced IL-18 receptor expression by various peripheral blood cell subsets as determined by anti-hIL-18R monoclonal antibody. Cell Immunol 189:135–143
13. Macatonia SE, Hosken NA, Litton M, Vieira P, Hsieh CS, Culpepper JA, Wysocka M, Trinchieri G, Murphy KM, O'Garra A (1995) Dendritic cells produce IL-12 and direct the development of Th1 cells from naive CD4+ T cells. J Immunol 154: 5071–5079
14. Munder M, Mallo M, Eichmann K, Modolell M (1998) Murine macrophages secrete interferon gamma upon combined stimulation with interleukin (IL)-12 and IL-18: a novel pathway of autocrine macrophage activation. J Exp Med 187:2103–2108
15. Murata Y, Ohteki T, Koyasu S, Hamuro J (2002) IFN-gamma and pro-inflammatory cytokine production by antigen-presenting cells is dictated by intracellular thiol redox status regulated by oxygen tension. Eur J Immunol 32:2866–2873
16. Nakanishi K, Yoshimoto T, Tsutsui H, Okamura H (2001) Interleukin-18 regulates both Th1 and Th2 responses. Annu Rev Immunol 19:423–474
17. Nomura A, Takada H, Jin CH, Tanaka T, Ohga S, Hara T (2001) Functional analyses of cord blood natural killer cells and T cells: a distinctive interleukin-18 response. Exp Hematol 29:1169–1176
18. Puddu P, Fantuzzi L, Borghi P, Varano B, Rainaldi G, Guillemard E, Malorni W, Nicaise P, Wolf SF, Belardelli F, Gessani S (1997) IL-12 induces IFN-gamma expression and secretion in mouse peritoneal macrophages. J Immunol 159:3490–3497
19. Reis e Sousa C, Hieny S, Scharton-Kersten T, Jankovic D, Charest H, Germain RN, Sher A (1997) In vivo microbial stimulation induces rapid CD40 ligand-independent production of interleukin 12 by dendritic cells and their redistribution to T cell areas. J Exp Med 186:1819–1829
20. Stober D, Schirmbeck R, Reimann J (2001) IL-12/IL-18-dependent IFN-gamma release by murine dendritic cells. J Immunol 167:957–965
21. Tominaga K, Yoshimoto T, Torigoe K, Kurimoto M, Matsui K, Hada T, Okamura H, Nakanishi K (2000) IL-12 synergizes with IL-18 or IL-1beta for IFN-gamma production from human T cells. Int Immunol 12:151–160
22. Yoshimoto T, Takeda K, Tanaka T, Ohkusu K, Kashiwamura S, Okamura H, Akira S, Nakanishi K (1998) IL-12 up-regulates IL-18 receptor expression on T cells, Th1 cells, and B cells: synergism with IL-18 for IFN-gamma production. J Immunol 161:3400–3407
23. Zhang T, Kawakami K, Qureshi MH, Okamura H, Kurimoto M, Saito A (1997) Interleukin-12 (IL-12) and IL-18 synergistically induce the fungicidal activity of murine peritoneal exudate cells against *Cryptococcus neoformans* through production of gamma interferon by natural killer cells. Infect Immun 65:3594–3599

Available online at www.sciencedirect.com
SCIENCE DIRECT®
Biochemical and Biophysical Research Communications 341 (2006) 1113–1118
BBRC
www.elsevier.com/locate/ybbrc

The effects of blood feeding and exogenous supply of tryptophan on the quantities of xanthurenic acid in the salivary glands of *Anopheles stephensi* (Diptera: Culicidae)

Bernard Okech [a,b,*], Meiji Arai [a], Hiroyuki Matsuoka [a]

[a] *Division of Medical Zoology, Department of Infection and Immunity, Jichi Medical School, Minamikawachi, Tochigi 329-0498, Japan*
[b] *Centre for Biotechnology, Research and Development (CBRD), Kenya Medical Research Institute (KEMRI), P.O. Box 54840, Nairobi, Kenya*

Received 24 December 2005
Available online 26 January 2006

Abstract

Xanthurenic acid (XA), produced as a byproduct during the biosynthesis of insect eye pigment (ommochromes), is a strong inducer of *Plasmodium* gametogenesis at very low concentrations. In previous studies, it was shown that XA is present in *Anopheles stephensi* (Diptera: Culicidae) mosquito salivary glands and that during blood feeding the mosquitoes ingested their own saliva into the midgut. Considering these two facts together, it is therefore likely that XA is discharged with saliva during blood feeding and is swallowed into the midgut where it exerts its effect on *Plasmodium* gametocytes. However, the quantities of XA in the salivary glands and midgut are unknown. In this study, we used high performance liquid chromatography with electrochemical detection to detect and quantify XA in the salivary glands and midgut. Based on the results of this study, we found 0.28 ± 0.05 ng of XA in the salivary glands of the mosquitoes, accounting for 10% of the total XA content in the mosquito whole body. The amounts of XA in the salivary glands reduced to 0.13 ± 0.06 ng after mosquitoes ingested a blood meal. Approximately 0.05 ± 0.01 ng of XA was detected in the midgut of nonblood fed *An. stephensi* mosquitoes. By adding synthetic tryptophan as a source of XA into larval rearing water (2 mM) or in sugar meals (10 mM), we evaluated whether XA levels in the mosquito (salivary glands, midgut, and whole body) were boosted and the subsequent effect on infectivity of *Plasmodium berghei* in the treated mosquito groups. A female specific increase in XA content was observed in the whole body and in the midgut of mosquito groups where tryptophan was added either in the larval water or sugar meals. However, XA in the salivary glands was not affected by tryptophan addition to larval water, and surprisingly it reduced when tryptophan was added to sugar meals. The *P. berghei* oocyst loads in the mosquito midguts were lower in mosquitoes fed tryptophan treated sugar meals than in mosquitoes reared on tryptophan treated larval water. Our results suggest that mosquito nutrition may have a significant impact on whole body and midgut XA levels in mosquitoes. We discuss the observed parasite infectivity results in relation to XA's relationship with malaria parasite development in mosquitoes.

Keywords: *Anopheles* mosquito; HPLC; Malaria; Salivary glands; Tryptophan; Xanthurenic acid

Xanthurenic acid (XA) is a gametocyte activating factor (GAF) that strongly induces *Plasmodium* gametogenesis [1,2]. XA is produced as a lateral reaction product during the ommochrome pathway of insect eye pigment synthesis [3]. The mosquito head has been demonstrated to contain a high amount of XA [4,5]. However, its distribution in mosquito organs that interact with *Plasmodium* gametocytes, such as the midgut, is unknown. Within the midgut lumen, the mature *Plasmodium* gametocytes that are ingested during blood feeding start gametogenesis [6,7]; therefore, the female mosquito midgut lumen should be rich in XA. In previous studies, GAF activity was found in the mosquito head, salivary glands, and midgut [8], however the identity or quantity of the GAF was not established.

During the blood feeding process, mosquitoes secrete saliva at the bite site to aid blood feeding by its dilation

* Corresponding author. Present address: University of Florida, 9505 Ocean Shore Blvd, St. Augustine, FL 32080, USA. Fax: +1 904 461 4008.
E-mail address: bokech@ufl.edu (B. Okech).

0006-291X/$ - see front matter © 2006 Elsevier Inc. All rights reserved.
doi:10.1016/j.bbrc.2006.01.079

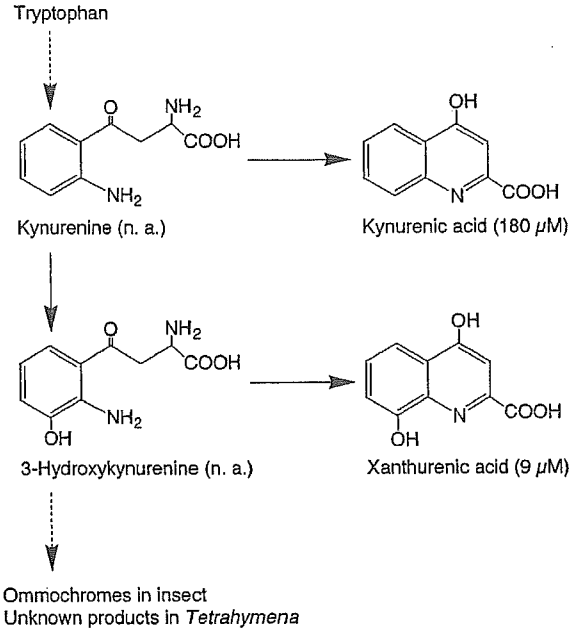

Fig. 1. The ommochrome biosynthesis pathway with chemical structures of the intermediates. The intermediates were tested for their microgametogenesis activity (see [23]) and are shown in parentheses. n.a, no activity observed. Dotted lines indicate that intermediate steps are omitted.

effect on blood vessels and anticoagulation effect on blood [9,10]. In previous studies, it was shown that mosquitoes ingest the secreted saliva with the blood into the midgut [11]. Considering these two facts together, it is likely that some XA is discharged with saliva during blood feeding and ingested to the midgut where it exerts its effect on *Plasmodium* gametogenesis. In our previous study, the XA levels in *An. stephensi* were qualitatively and semi-quantitatively evaluated using the bioassay method [8]. In the present study, we have employed a sensitive, qualitative, and quantitative detection system, the high performance liquid chromatography with electrochemical detection (HPLC-ED) [12], to quantify XA in the salivary glands and midgut of *An. stephensi* mosquitoes. We further evaluated the pre- and post-blood feeding XA levels in the salivary glands; and by boosting the synthesis of XA through addition of synthetic tryptophan (see Fig. 1) into larval rearing water or into sugar meals, we also evaluated whether ingestion of tryptophan from larval water or in sugar meals affected XA amounts in the salivary glands and midgut, and on *P. berghei* parasite infection in *An. stephensi* mosquitoes. Information on the XA quantities in mosquitoes is important in the attempts to identify new targets to prevent or interfere with gametogenesis so as to interrupt malaria parasite development in mosquitoes.

Materials and methods

Mosquitoes used in the experiments. *Anopheles stephensi* mosquitoes (SDA 500 strain) were used in all the experiments. Mosquitoes were reared according to standard protocols used in the insectary within the Division of Medical Zoology, Jichi Medical School, Japan. Briefly, larvae were reared at densities not exceeding 200 per 400 mL of water. At least once everyday, they were fed on a pinch of ground Japanese carp fish food (Kyorin Food Industries Ltd, Himeji, Japan) that was sprinkled over the surface of water. Larval rearing water was changed every 3 days until pupae formed. Pupae were collected and transferred to nylon meshed cages where emerging adult mosquitoes had access to 5% fructose sugar meals. Mosquitoes were used 5 days after emergence. For the determination of XA in whole body, male and female mosquitoes were collected separately and placed in vials containing 500 μl of 0.4 M formic acid and stored at −20 °C. And for the determination of XA in salivary glands and midguts, female mosquitoes were immobilized by chilling on ice and their salivary glands (~50–100 pairs) and midguts (~30–50) were isolated by dissection and immediately placed in cold 0.4 M formic acid. They were then stored at −20 °C until processing for HPLC-ED analysis.

Effect of blood feeding. Two groups of 5-day-old female mosquitoes were used in this experiment, one group (experimental) was offered an opportunity to feed for 15 min on a BALB/c mouse that was anesthetized with an intramuscular injection of a mixture of xylazine (Bayer UK Limited, St. Edmunds, UK) and ketamine (Sankyo, Tokyo, Japan) at the doses of 0.2 mg/kg and 2 mg/kg bodyweight, respectively, while the other group (used as a control) was not offered a blood meal. In the blood fed group, engorged mosquitoes were collected and immobilized on ice. An equal number of control mosquitoes were also immobilized in the same way. In this immobilized state, the salivary glands of the mosquitoes were isolated by dissection and transferred to 100 μl of chilled 0.4 M formic acid in Eppendorf tubes. Fifty to hundred pairs of salivary glands were dissected and processed further for HPLC analysis. The experiment was repeated five times.

Exogenous supply of synthetic L-*tryptophan in larval rearing water.* Two groups of 150 mosquito larvae at the second instar stage were each set aside; the experimental group was placed in 400 mL of rearing water containing 2 mM L-tryptophan (Sigma Chemical, St. Louis, MO, USA) and the control group placed in normal water without tryptophan. The two groups were then reared according to the standard protocols of the insectary. At each subsequent developmental stage (L3, L4, and Pupae), 5–10 mosquitoes were collected, transferred to Eppendorf tubes containing 0.4 M formic acid, and processed further for HPLC-ED analysis. Emerging adult mosquitoes from the experimental and control groups were separately kept in cages where they had access to 5% fructose solution. After 5 days, whole bodies of male (~10) and female (~10) mosquitoes were put in 0.4 M formic acid and processed HPLC-ED analysis. The mosquitoes used in the experiment were of similar size in both groups. In addition, salivary glands and midguts were obtained from female mosquitoes as described above and processed for HPLC-ED analysis. The remaining mosquitoes were offered a blood meal from a gametocytemic BALB/c mouse, which was anesthetized and put on the top of the two cages. The two groups of mosquitoes were able to feed on the same mouse from beneath the nylon mesh. Fourteen days after blood feeding, the mosquitoes were dissected and the number of oocysts in the midgut was determined by observation under 40× magnifications using a light microscope [13].

Exogenous supply of synthetic L-*tryptophan in fructose solution.* Emerging mosquitoes from normal water were collected, divided into two groups, and held separately in cages. In one of the cages (experimental), the mosquitoes had access to 5% fructose sugar plus 10 mM tryptophan while the other (control) mosquitoes had 5% fructose solution only. They were kept under these conditions for 4 days. A day before being used in experiments, they were each provided fresh solution of 5% fructose. Male (~10) and female (~10) mosquitoes were processed for analysis in HPLC-ED. In addition, the salivary glands and midguts of females from both groups were also dissected and processed for analysis in HPLC-ED. The remaining mosquitoes were offered blood meal from a gametocytemic BALB/c mouse and after 14 days were dissected and assessed for oocyst infection as described above.

Processing of mosquito samples for HPLC-ED analysis. The stored *An. stephensi* whole body samples were homogenized in 500 μl of 0.4 M formic acid using a glass homogenizer on ice and sonicated for 2 min using an ultrasonicator. The stored salivary glands and midguts were first washed by centrifugation (15 s at 2000*g*) and then processed by adding 100 μl of chilled 0.4 M formic acid and then centrifuging the samples for 10 min at 15,000*g*. They were then homogenized using a micro-homogenizer and sonicated for 2 min using an ultrasonicator as described above. The mosquito samples (whole body, salivary gland, and midgut) were then centrifuged (15 min at 2000*g*) and the supernatants were collected and ultrafiltered through a series of molecular weight cut-off filters of 100, 30, and 5 kDa (VivaScience AG, Hannover, Germany). The flow-through filtrate from the 5 kDa molecular weight cut-off filter was finally used in the HPLC-ED analysis.

The identification and quantification of xanthurenic acid in mosquito samples by HPLC-ED. HPLC-ED can be used in the identification and quantification of XA [12]. The HPLC-ED apparatus employed in our study consisted of a PU-980 Intelligent HPLC pump (Jasco, Tokyo, Japan), an injector (Rheodyne, CA, USA) fitted with a 20 μl sample loop, and an ECD-300 electrochemical detector (EiCom, Tokyo, Japan). A reverse-phase 5 μm C-18 column (4.6 × 150 mm) (Tosoh Biosciences, Japan) was used for the separation of compounds in mosquito samples. The mobile phase consisted of 0.1 M citrate buffer (0.1 M citric acid, pH 3.0) containing 8% acetronitrile and sometimes with 1.8 mM octyl sulfate (Sigma). A flow rate of 0.6 ml/min was used during chromatography. By loading 20 μl of mosquito sample using a Hamilton syringe, we detected several peaks and identified among them an XA peak. The identification of XA peak was based on its retention time in the chromatogram of synthetic XA (Sigma). Additional confirmation of the identity of XA in the salivary glands sample was based on its behavior in the presence of octyl sulfate, spiking with synthetic XA, and XA peak shifts at various electrode potentials (redox potential on the electrode was adjusted at 50 mV intervals between 650 and 850 mV). These HPLC-ED procedures have been applied before in the decisive identification of XA in larval and adult insect tissues [14]. During the analysis, the amount of sample injected and the sensitivity of the detector remained constant. The quantification of XA was achieved by estimation from a standard curve generated by injecting increasing amount of XA and measuring peak heights. The column sensitivity was maintained by washing and storage in 50% methanol after every experiment.

Statistical analysis. The Student's *t* test was applied to test the differences in salivary gland XA levels before and after blood feeding. The differences in the quantities of XA in whole body, midgut, and salivary glands after addition of tryptophan in larval water or sugar meals was also tested by Student's *t* test. The Mann–Whitney *U* test was applied to test differences in the oocyst numbers in the tryptophan treated versus control group.

Results

Identity and quantity of XA in mosquito samples

Upon loading mosquito sample in the HPLC-ED, several peaks were observed and among them an XA peak was identified (Fig. 2). The identity was confirmed as described previously in the Materials and methods section. The other peaks not conforming to the properties of synthetic XA were ignored. The amount of XA detected in the salivary glands of *An. stephensi* was 0.28 ± 0.05 ng which represented 10% of the whole body XA content (Table 1). In separate experiments, we determined the midgut amount of XA in nonblood fed mosquitoes to be 0.05 ± 0.02 ng and in the whole body of female mosquitoes to be about 2.8 ± 1.9 ng (Table 1).

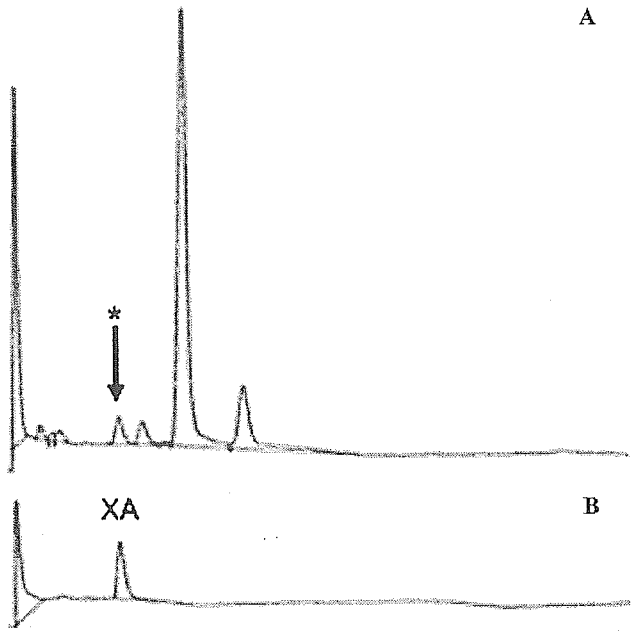

Fig. 2. The identification of xanthurenic acid in the salivary glands of *An. stephensi* (A) based on its retention time when compared to synthetic xanthurenic acid (B). (A) Chromatogram of salivary gland sample and (B) synthetic XA. *The XA peak is the crude salivary gland sample.

Table 1
The contribution of salivary gland to the whole body XA amount

Mosquito part	Volume (μl) (% of whole body)	XA quantity (ng) (% of whole body)	Concentration index[a]
Whole body	2.3 (100%)	2.8 (100%)	1.2
Midgut	0.13 (5.7%)	0.05 (2%)	0.4
Salivary glands	0.007 (0.3%)	0.28 (10%)	40

[a] Concentration index is a ratio to indicate the XA quantity in the volume of the mosquito body. It is the ratio of XA quantity to the volume.

Effect of blood feeding on xanthurenic acid quantities in the salivary glands

When mosquitoes feed on blood, the salivary glands shrink due to the secretion of saliva. Our study was concerned with the amount of XA discharged with the saliva which might be swallowed to the midgut to effect gametogenesis of *Plasmodium*. We found that the amount of XA in the salivary glands of mosquitoes significantly (*t* test: $P < 0.05$) reduced after blood feeding to 0.13 ± 0.06 ng representing a drop of 54% (Fig. 3). The amount of XA in the midgut after blood feeding was not determined in this study as it would be difficult to differentiate whether the XA is from salivary glands or blood meal [23,24].

Effect of tryptophan supplementation

Xanthurenic acid is a downstream metabolite of the parent amino acid tryptophan. We hypothesized that addition of synthetic tryptophan to mosquitoes would boost the content of XA in mosquito tissues. The addition of trypto-

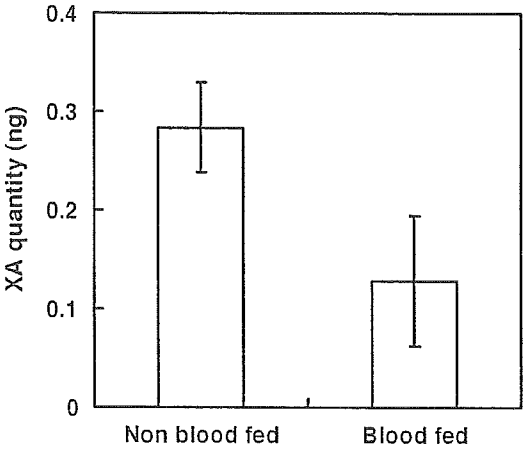

Fig. 3. The effect of blood feeding on the amounts of xanthurenic acid (ng) in a single pair of salivary glands of *An. stephensi* mosquitoes estimated using HPLC with electrochemical detection ($n = 5$).

phan in larval water resulted in a high increase in the XA content in the immature mosquito stages (L3, L4, and pupae) in the treated groups as compared to the controls. The whole body XA amount in females was significantly higher than in controls when tryptophan was added to larval water (2.8 ± 1.9 *vs.* 6.4 ± 1.6 ng) or in sugar meals (2.8 ± 1.9 *vs.* 4.9 ± 0.5 ng), while no significant difference was observed in male mosquitoes (Table 2). This result shows that female mosquitoes produced more XA when exposed to high tryptophan conditions than male mosquitoes. Furthermore in the females, the midgut XA amount was significantly higher in tryptophan added groups, both in the larval water and sugar meal experiments (Table 2). Salivary gland XA amounts did not significantly increase by addition of tryptophan to larval water but it surprisingly reduced to 0.14 ± 0.07 ng when tryptophan was added to sugar meals, a decrease of approximately 51% as compared to controls (Table 2).

Table 2
The effect of addition of tryptophan in the larval water or in fructose sugar meals on XA amounts (ng) in *An. stephensi* whole body, midgut, and salivary glands

Mode of adding tryptophan	Without tryptophan	With tryptophan	Probability
In larval water			
Males	2.0 ± 1.2	2.1 ± 0.7	NS[a]
Females	2.8 ± 1.9	6.4 ± 1.6	$P < 0.05$
Midgut	0.05 ± 0.01	0.11 ± 0.05	$P < 0.05$
Salivary glands	0.28 ± 0.05	0.30 ± 0.05	NS[a]
In fructose solution			
Males	2.0 ± 1.2	2.2 ± 0.2	NS[a]
Females	2.8 ± 1.9	4.9 ± 0.5	$P < 0.05$
Midgut	0.05 ± 0.01	0.10 ± 0.03	$P < 0.05$
Salivary glands	0.28 ± 0.05	0.14 ± 0.07	$P < 0.05$

Values are given in nanograms ± SEM.
[a] NS, not significant.

Effect of tryptophan supplementation on P. berghei infections in An. stephensi

The induction of gametogenesis in vivo specifically requires a drop in temperature and a second factor which is XA. Because XA is derived only from the metabolism tryptophan, its availability in mosquito body might have increased in vivo contents of XA to affect parasite development. In our experiments, *P. berghei* infections in mosquitoes from the larval water experiments were not significantly different in the group supplemented with tryptophan compared to the control (Figs. 4A and B) and the infection results when pooled together were almost the same. For the sugar meals experiments, the number of oocysts in mosquitoes from the tryptophan treated group was lower than in the control group in all the three separate infection experiments (Figs. 4C–E). The differences in oocyst numbers were significantly different ($P < 0.05$) when the oocyst data in all experiments were pooled.

Discussion

We have demonstrated the XA distribution in *An. stephensi* mosquito whole body including the midgut and salivary glands by using HPLC-ED. The sensitivity of the HPLC-ED, which is estimated 10^{-12}–10^{-13} g/ml (pico scale level), makes this method ideal for the identification and quantification of XA in a small mosquito part like the salivary glands. We have estimated the quantities of XA in the salivary glands to be 0.28 ng which accounts for 10% of whole body XA content. We measured the volume of the salivary glands at 0.007 μl, and when compared to the whole mosquito body (2.3 μl), it is only 0.3%, yet 10% of whole body XA is found here. XA level in the salivary glands of mosquitoes reduced after blood feeding, suggesting that the release of saliva that corresponds to reduced salivary gland volume [15] is the likely cause of the drop in the XA amount in the salivary glands. The salivary gland shrinkage after blood feeding has been estimated at between 50 and 60% [16] and is quite consistent with the XA reduction seen in this study. This suggests that saliva ingested during blood feeding [11] contributes XA in the midgut. The reason and mechanism behind the relatively high concentration of XA in the salivary glands itself warrants further investigation.

We have also shown that the exogenous supply of tryptophan, either via larval water or adult sugar meals, resulted in the accumulation of XA only in female mosquitoes, suggesting that XA accumulation may be sex linked. The data also suggest that the amounts of XA in the mosquito body may vary depending on the nutritional conditions of mosquitoes. This is important considering that in nature there are natural diets such as nectar [17], honey dew [18], and pollen [19] available to wild mosquito populations that are sources of tryptophan. In addition, we observed an increase of XA amounts in the midgut, where *Plasmodium* gametocytes make first contact. On the other hand, the provision of tryp-

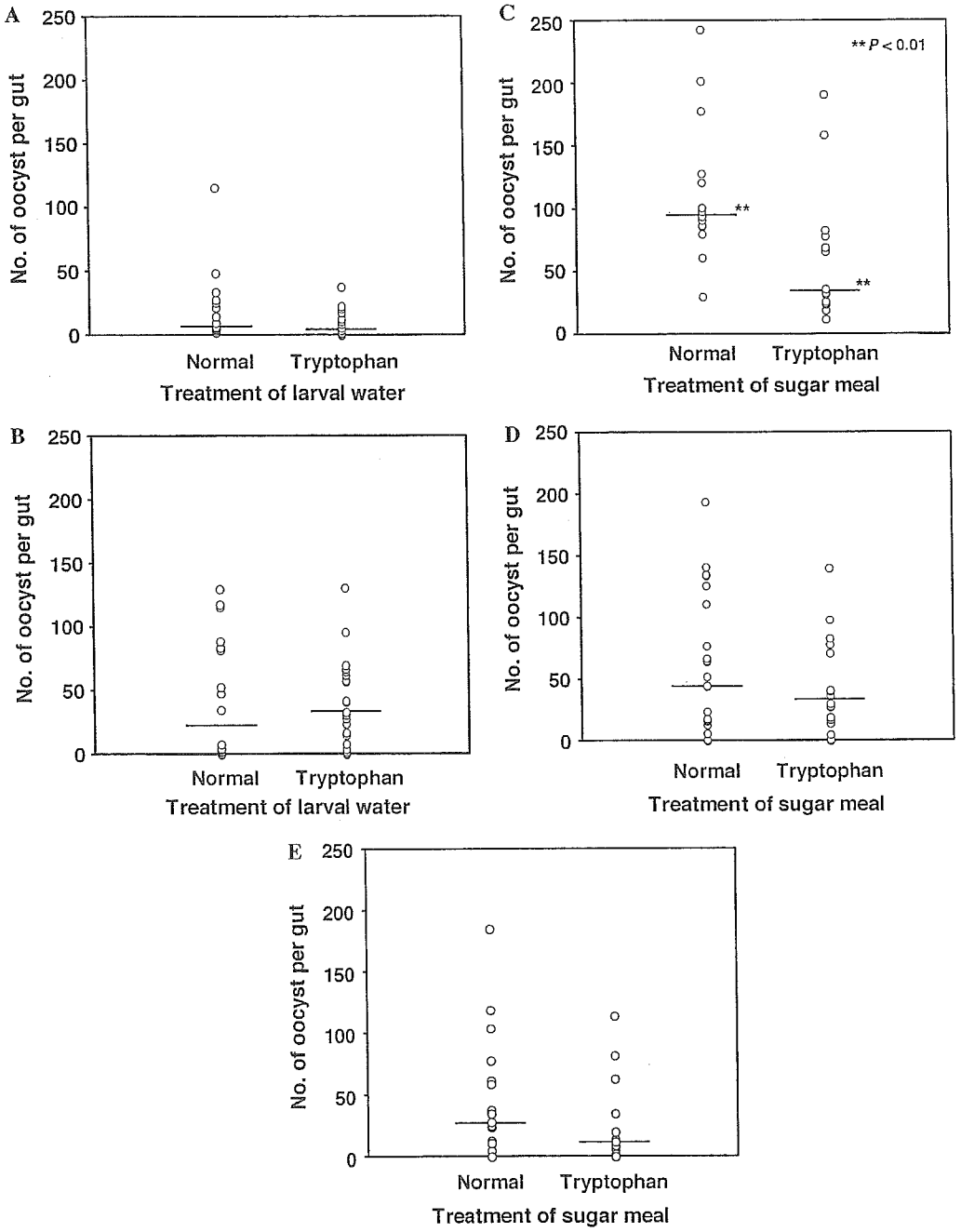

Fig. 4. *P. berghei* oocyst infectivity of mosquitoes treated with tryptophan in larval water (A,B) or in sugar meals (C, D, and E). The median values are shown with a line crossing the scatter plots.

tophan through sugar meals surprisingly led to the reduction of the XA amount in the saliva as opposed to whole body and midgut. Although this reduction may be as a result of the release of saliva during sugar feeding [16], it may also have been due to 5-hydroxytryptamine (5-HT), a tryptophan metabolite that is known to induce salivation in insects including mosquitoes [20,21]. However, it remains to be studied whether tryptophan itself or other amino acids induce any salivation in mosquitoes. The increase of XA in all the mosquito stages (L2, L3, L4, pupae, and adults) suggests that XA molecules are cummulatively retained in the mosquito body tissues after it is synthesized as larvae grows. This result may provide clues of the processes involved in the accumulation of XA in the salivary glands.

The addition of tryptophan in sugar meals resulted in higher midgut XA levels and lower salivary gland XA. Mosquitoes offered tryptophan in fructose had low numbers of oocyst infection in the midgut. Although this may have been as a result of the small quantity of XA available for the parasites in the midgut (see below), it is not known whether synthetic tryptophan may have had negative effects on parasite development. It is noteworthy to mention that other metabolites of tryptophan have been tested on *P. berghei* exflagellation assays and it has been shown

that XA is the most bioactive at very low concentrations compared to other tryptophan metabolites [23]. Therefore, the effects of other amino acids and their metabolites on *P. berghei* infectivity, although important, were not studied because it was beyond the scope of our objectives. Estimation of the XA quantities available to the parasite in the mosquito midgut indicated that for the tryptophan treated larval water, there was a twofold increase in the XA available in the midgut (6.4 μM), assuming that 50% of the salivary XA was transferred to the midgut, as compared to the control (3.0 μM). This is based on the estimation that *An. stephensi* mosquitoes ingest a blood mean volume 2 μl [22]. For the sugar plus tryptophan fed group, there was a slightly higher level of XA available in the midgut (3.2 μM) as compared to the controls (2.5 μM). It has been demonstrated that *P. berghei* requires 9 μM XA to achieve half maximal exflagellation activity [1,23] and the amount of XA quantified in this study would be insufficient. However, it should be noted that the levels of XA quantified in this study are estimations of the salivary gland sources of XA and other sources, e.g., blood meal [24] and other GAF factors may be involved in the stimulation of gametogenesis in the mosquito midgut [23]. The amounts of XA we have estimated in this study are sufficiently abundant to induce 50% maximal exflagellation responses for *P. falciparum* which requires only 2 μM XA [23]. Importantly, this study shows that environmental resources may affect the quantities of XA molecule that is a critical inducer for the initiation of the sexual phase of malaria development in the mosquitoes.

Acknowledgments

We acknowledge Japan International Co-operation Agency (JICA) and Kenya Medical Research Institute (KEMRI) for providing support to BAO. Much appreciation to the laboratory members of the Division of Medical Zoology, Jichi Medical School, for logistical support.

References

[1] O. Billker, V. Lindo, M. Panico, A.E. Etienne, T. Paxton, A. Dell, M. Rogers, R.E. Sinden, H.R. Morris, Identification of xanthurenic acid as the putative inducer of malaria development in the mosquito, Nature 392 (1998) 289–292.

[2] G.E. Garcia, R.A. Wirtz, J.R. Barr, A. Woolfitt, R. Rosenberg, Xanthurenic acid induces gametogenesis in *Plasmodium*, the malaria parasite, J. Biol. Chem. 273 (1998) 12003–12005.

[3] A. Sarker, F.H. Collins, Eye color genes for the selection of transgenic insects, in: Alfred M. Handler, Anthony A. James (Eds.), Insects Transgenesis: Methods and Applications, CRC Press, NY, 2000, pp. 79–91.

[4] M.M. Nijhout, R. Carter, Gamete development in malaria parasites: bicarbonate-dependent stimulation by pH in vitro, Parasitology 76 (1978) 39–53.

[5] G.E. Garcia, R.A. Wirtz, R. Rosenberg, Isolation of a substance from the mosquito that activates *Plasmodium* fertilization, Mol. Biochem. Parasitol. 88 (1997) 127–135.

[6] J.C. Beier, Malaria parasite development in mosquitoes, Ann. Rev. Entomol. 43 (1998) 519–543.

[7] R.E. Sinden, Molecular interactions between *Plasmodium* and its insect vectors, Cell. Microbiol. 4 (2002) 713–724.

[8] M. Hirai, J. Wang, S. Yoshida, A. Ishii, H. Matsuoka, Characterization and identification of exflagellation-inducing factor in the salivary gland of *Anopheles stephensi* (Diptera: Culicidae), Biochem. Biophys. Res. Commun. 287 (2001) 859–864.

[9] J.M. Ribeiro, Role of saliva in blood-feeding by arthropods, Ann. Rev. Entomol. 32 (1987) 463–478.

[10] D.E. Champagne, The role of salivary vasodilators in blood feeding and parasite transmission, Parasitol. Today 10 (1994) 430–433.

[11] E. Luo, H. Matsuoka, S. Yoshida, K. Iwai, M. Arai, A. Ishii, Changes in the salivary proteins during blood feeding and detection of salivary proteins in the midgut after feeding in the malaria vector *Anopheles stephensi* (Diptera: Culicidae), Med. Entomol. Zool. 51 (2000) 13–20.

[12] J. Li, G. Li, Identification of 3- hydroxykynurenine and xanthurenic acid and the quantification of 3-hydroxykynurenine transaminase activity using HPLC with electrochemical detection, J. Liq. Chrom. R. T. 21 (1998) 1511–1523.

[13] S. Yoshida, D. Ioka, H. Matsuoka, H. Endo, A. Ishii, Bacteria expressing single-chain immunotoxin inhibit malaria parasite development in mosquitoes, Mol. Biochem. Parasitol. 113 (2001) 89–96.

[14] J. Li, G. Li, Transamination of 3-hydroxykynurenine to produce xanthurenic acid: a major branch pathway of tryptophan metabolism in the mosquito, *Aedes aegypti*, during larval development, Insect Biochem. Mol. Biol. 27 (1997) 859–867.

[15] M. Matsuoka, H. Matsubara, P. Widhet, T. Hashimoto, A. Ishii, Y. Sato, K. Ando, Y. Chinzei, Depletion of the salivary gland proteins in *An. stephensi* (Diptera: Culicidae) on blood feeding, and induction of antibodies to the proteins in mice being fed, Med. Entomol. Zool. 48 (1997) 211–218.

[16] A.N. Clements, The biology of mosquitoes, Vol. 1. Development, Nutrition and Reproduction, Chapman & Hall, London, 1992.

[17] M.H. Haydak, Honey bee nutrition, Ann. Rev. Entomol. 15 (1970) 143–156.

[18] J. Woodring, R. Wiedemann, M.K. Fischer, K.H. Hoffmann, W. Völkl, Honeydew amino acids in relation to sugars and their role in the establishment of ant-attendance hierarchy in eight species of aphids feeding on tansy (*Tanacetum vulgare*), Physiol. Entomol. 29 (2004) 311–319.

[19] Y. Ye-Ebiyo, R.J. Pollack, A. Spielman, Enhanced development in nature of larval *Anopheles arabiensis* mosquitoes feeding on maize pollen, Am. J. Trop. Med. Hyg. 63 (2000) 90–93.

[20] M.G. Novak, W.A. Rowley, Serotonin depletion affects blood-feeding but not host-seeking ability in *Aedes triseriatus* (Diptera: Culicidae), J. Med. Entomol. 31 (1994) 600–606.

[21] M.G. Novak, J.M. Ribeiro, J.G. Hildebrand, 5-hydroxytryptamine in the salivary glands of adult female *Aedes aegypti* and its role in regulation of salivation, J. Exp. Biol. 198 (1995) 167–174.

[22] R.E. Sinden, *Plasmodium* differentiation in the mosquito, Parassitologia 41 (1999) 139–148.

[23] M. Arai, O. Billker, H.R. Morris, M. Panico, M. Delcroix, D. Dixon, S.V. Ley, R.E. Sinden, Both mosquito-derived xanthurenic acid and a host blood-derived factor regulate gametogenesis of *Plasmodium* in the midgut of the mosquito, Mol. Biochem. Parasitol. 116 (2001) 17–24.

[24] S.A. Williams, J.A. Monti, L.R. Boots, P.E. Cornwell, Quantitation of xanthurenic acid in rabbit serum using high performance liquid chromatography, Am. J. Clin. Nutr. 40 (1984) 159–167.

Available online at www.sciencedirect.com
SCIENCE DIRECT®
Molecular & Biochemical Parasitology 140 (2005) 13–21
MOLECULAR & BIOCHEMICAL PARASITOLOGY

Erythrocyte surface glycosylphosphatidyl inositol anchored receptor for the malaria parasite

Thanaporn Rungruang[a], Osamu Kaneko[a,*], Yoshiko Murakami[b], Takafumi Tsuboi[a,c], Hiroshi Hamamoto[d], Nobuyoshi Akimitsu[d], Kazuhisa Sekimizu[d], Taroh Kinoshita[b], Motomi Torii[a]

[a] *Department of Molecular Parasitology, Ehime University School of Medicine, Toon, Ehime 791-0295, Japan*
[b] *Department of Immunoregulation, Research Institute for Microbial Diseases, Osaka University, Suita, Osaka 565-0871, Japan*
[c] *Cell-Free Science and Technology Research Center, Ehime University, Matsuyama, Ehime 790-8577, Japan*
[d] *Laboratory of Developmental Biochemistry, Graduate School of Pharmaceutical Sciences, The University of Tokyo, Tokyo 113-0033, Japan*

Received 29 August 2004; received in revised form 3 November 2004; accepted 4 November 2004
Available online 23 December 2004

Abstract

Parasitophorous vacuole formation is a critical step for the successful invasion of host erythrocytes by the malaria parasite. Rhoptry proteins are believed to have essential roles in vacuole formation, although their biological roles are poorly understood. To understand the molecular interactions between parasite rhoptry proteins and the erythrocyte during invasion, we have characterized the binding specificity of the high molecular mass rhoptry protein (RhopH) complex to erythrocytes using the rodent malaria parasite, *Plasmodium yoelii*. RhopH complex binding to erythrocytes was species-specific, observed with mouse but not rabbit or human erythrocytes. Binding is abolished following treatment of erythrocytes with trypsin or chymotrypsin. Because host cell cholesterol-rich membrane domains are recruited into the nascent parasitophorous vacuole, we evaluated a possible role of RhopH complex binding to the cholesterol-rich membrane domain-associated glycosylphosphatidyl inositol (GPI)-anchored protein. Using chimeric mice harboring GPI-deficient erythrocytes, RhopH complex binding to GPI-deficient mouse erythrocytes was undetectable, indicating involvement of GPI-anchored protein in *Py*RhopH complex binding. Furthermore, a significant reduction of *P. yoelii* parasite infection of GPI-deficient erythrocytes was observed in vivo, probably due to inefficient invasion. We conclude that the major erythrocyte receptor for *Py*RhopH complex is a protein attached to the erythrocyte surface via GPI-anchor and that GPI-deficient erythrocytes are resistant to *P. yoelii* invasion.

Keywords: Erythrocyte; GPI anchor; Invasion; Malaria; *Plasmodium yoelii*

1. Introduction

Malaria is one of the most prevalent and deadly global infectious diseases and is caused by the obligate intraerythrocytic stages of the protozoan parasite, *Plasmodium*. To facilitate erythrocyte invasion, *Plasmodium* merozoites discharge the contents of apical organelles called rhoptries that are involved in the formation of an intraerythrocytic parasitophorous vacuole in which the parasites reside and develop. The parasitophorous vacuole membrane (PVM) contains erythrocyte proteins found in detergent-resistant membrane [e.g., Duffy antigen receptor for chemokines (DARC) and glycosylphosphatidylinositol (GPI)-anchored proteins], but excludes most transmembrane proteins (e.g., glycophorin A) [1].

Abbreviations: DARC, Duffy antigen receptor for chemokines; EDTA, ethylenediaminetetraacetic acid; GPA, glycophorin A; mAb, monoclonal antibody; PBS, phosphate buffered saline

* Corresponding author. Tel.: +81 89 960 5286; fax: +81 89 960 5287.
E-mail address: okaneko@m.ehime-u.ac.jp (O. Kaneko).

0166-6851/$ – see front matter © 2004 Elsevier B.V. All rights reserved.
doi:10.1016/j.molbiopara.2004.11.017

A number of rhoptry proteins have been identified, including a complex of high molecular mass proteins containing three distinct polypeptides, RhopH1, RhopH2 and RhopH3 (the RhopH complex) [2–5]. The RhopH genes have been cloned from the human malaria parasite, *Plasmodium falciparum*, as well as the rodent malaria parasite, *Plasmodium yoelii* [6–10]. The *P. falciparum* RhopH (*Pf*RhopH) complex binds erythrocytes and distributes into the erythrocyte and parasitophorous vacuolar membranes [11,12]. *Pf*RhopH appears to be essential for parasite development: antibodies against the *Pf*RhopH complex partially inhibit growth of *P. falciparum* in vitro and in vivo [13–15], and attempts to disrupt the *Pf*RhopH3 gene locus were unsuccessful, suggesting a resulting lethal phenotype [16]. Taken together, these results strongly indicate that the RhopH complex has a critical role in erythrocyte invasion; however, the molecular interactions of this protein complex are poorly understood. For example, erythrocyte surface binding of the *P. falciparum Pf*RhopH complex was observed only with erythrocytes of the non-susceptible mouse, but not those of the susceptible human host, for which the RhopH complex receptor has not been identified.

To explore a biological role of the rhoptry proteins, we are focusing to characterize the erythrocyte receptors for the RhopH complex using a rodent malaria parasite. In this report we describe a flow cytometric-based erythrocyte binding assay and show that the *P. yoelii* RhopH complex specifically binds to erythrocytes of a susceptible mouse host. Using chimeric mice harboring GPI-deficient erythrocytes, we further show a possible role of the GPI-anchored protein for RhopH complex binding and determine that GPI-deficient erythrocytes are resistant to *P. yoelii* infection.

2. Materials and methods

2.1. Parasites and parasite extracts

Parasite infected blood was collected from *P. yoelii* 17X (lethal)-infected BALB/c mice and leukocytes were removed by passing through a CF11 column. Schizont-stage parasites were enriched by differential centrifugation over 50% Percoll (Amersham Pharmacia Biotech Inc., UK), washed twice in phosphate buffered saline (PBS), pH 7.4, and stored at −80 °C. Parasite proteins were extracted by three times repeated freeze-thaw at −80 °C from schizont-rich pellets in PBS, pH 7.4, containing protease inhibitors [PI; 1 μg ml^{-1} of leupeptin, 1 μg ml^{-1} of pepstatin A, 100 μM 4-(2-aminoethyl)benzenesulfonyl fluoride hydrochloride] and 1 mM EDTA (ethylenediaminetetraacetic acid), and a soluble fraction was obtained by centrifugation at 21,600 × *g* for 10 min to make a final concentration used for erythrocyte binding assays corresponding to 1×10^7 parasites μl^{-1}.

2.2. Monoclonal antibodies

The monoclonal antibodies mAb#25 (IgG1), #32 (IgG2b) and #16 (IgG1) recognizing *P. yoelii* RhopH2, RhopH3 and yPys25, respectively, were described [8,17].

2.3. Erythrocytes

Female BALB/c, DBA/2 and C57BL/6 (B6) mice were obtained from Charles River Japan Inc. GPA wild type (GPA$^{+/+}$) and knockout (GPA$^{-/-}$) mice and DARC wild type (DARC$^{+/+}$) and knockout (DARC$^{-/-}$) mice were generated and maintained in Tokyo University as described [18,19]. Mice harboring GPI-deficient erythrocytes were generated and maintained in Osaka University. Briefly, B6 mice were lethally irradiated and fetal liver cells were transplanted from mice with a disrupted *Pig-a* gene locus, which was essential for the GPI biosynthesis. Control mice were generated in a similar manner except that bone marrow was transplanted from a normal mouse [20]. Mouse blood was collected from tail snip bleeds into an excess amount of PBS containing 50 mM EDTA, washed extensively with PBS to remove serum and buffy coat, stored in PBS containing 1% bovine serum albumin (BSA), and used for binding assays within 1 day of preparation. Erythrocytes were also collected from two rabbits (JW/CSK; Japan SLC Inc., Japan) and two human donors (O-type/Rh-positive) by venous puncture and processed in a similar manner.

2.4. Erythrocyte enzyme treatments

Erythrocytes were incubated in RPMI1640 medium without sodium bicarbonate (designated as RPMI1640) with 1 mg ml^{-1} trypsin (Sigma, St. Louis, MO) or 1 mg ml^{-1} chymotrypsin (Sigma) for 2 h at 37 °C with gentle rocking. The erythrocytes were then washed once with RPMI1640, incubated with 1 mg ml^{-1} soybean trypsin inhibitor (STI; Sigma) or 10 mM *N*-p-Tosyl-L-phenylalanine chloromethyl ketone (TPCK; Sigma), respectively, for 10 min at room temperature (RT) with gentle rocking, and washed once with RPMI1640. Control erythrocytes were treated with STI or TPCK only.

Erythrocytes were also incubated with 100 or 200 mU ml^{-1} neuraminidase (1 U ml^{-1}; *Vibrio cholera*, CalBiochem, San Diego, CA) for 2 h at 37 °C and washed three times with RPMI1640. Two control treatments were devised as follows. In one tube, erythrocytes were incubated with a corresponding volume of the buffer. In a second tube, EDTA with a final concentration of 10 mM was added in addition to the neuraminidase solution, to inactivate neuraminidase activity by chelating calcium. Fluorescein isothiocyanate (FITC)-conjugated wheat germ agglutinin (WGA) recognizing *N*-acetylneuraminic acid (NANA) residues was used to monitor erythrocyte surface desialylation.

2.5. Erythrocyte binding assay

Approximately 1×10^7 erythrocytes were incubated in 100 μl of PBS with 10% BSA for 1 h, washed once with PBS, and further incubated in 100 μl of PBS containing 20 μl of *P. yoelii* extract for 30 min at RT, if specific volumes were not indicated. After centrifugation, the mixture was divided into erythrocyte pellets and supernatants containing unbound *P. yoelii* RhopH complexes. Supernatants were saved for later analysis to monitor RhopH complex protein degradation. Erythrocyte pellets were washed once with PBS and incubated with 1 μg of mAb#25, #32, or #16 for 15 min on ice, washed once with PBS, and incubated with 1 μg of FITC-conjugated goat anti-(mouse IgG and IgM) antibody (Biosource Int, Camarillo, CA) for 15 min on ice in 1 ml of PBS. After washing once with PBS, erythrocyte surface fluorescence was detected by flow cytometry. All experiments were done with duplicated samples and enzyme-treated erythrocytes were used in binding assays in the same day as treatment.

To distinguish GPI-deficient and GPI-positive erythrocyte populations, erythrocyte surface GPI anchor-associated CD24 was stained with rat anti-mouse CD24 mAb (BD Biosciences, San Jose, CA) and streptavidin-phycoerythrin (PE)-Cy5 (BD Biosciences). Erythrocytes from control normal mice were stained with or without anti-CD24 mAb and used as positive controls.

2.6. Flow cytometry analysis

Erythrocytes (1×10^7) were suspended in 1 ml of PBS and surface fluorescence intensities were measured by flow cytometry using a FACSCalibur™ (Becton Dickinson, NJ) flow cytometer and analyzed using the CellQuest™ software. First, single-parameter histograms were set for FITC fluorescence of cells within the scatter gate, with a gate set on the major erythrocyte population, and conditions were adjusted using untreated erythrocytes. Then, the geometric means of the fluorescence intensities were obtained for 10,000 erythrocytes incubated with or without *P. yoelii* extracts. Binding of the RhopH complex to the erythrocyte surface were given as a value obtained by dividing the geometric mean of fluorescence intensity of the experimental samples (with extract; INT_{exp}) by that of the control samples (without extract; INT_{ctl}).

For dual staining with FITC and PE-Cy5, erythrocytes were divided into two populations by PE-Cy5-fluorescence intensity and geometric mean of FITC fluorescence intensity increase were measured in these two populations independently.

2.7. SDS-PAGE, Western blot analysis, and immunoprecipitation

Parasite extracts were separated by electrophoresis on a 5–20% gradient polyacrylamide gel (ATTO, Japan) under non-reducing conditions and transferred to 0.22 μm PVDF membranes (Bio-Rad, Hercules, CA). Proteins were detected by immunostaining with corresponding antibodies, followed by horseradish peroxidase-conjugated goat antibody (anti-mouse IgG and IgM; Biosource Int) and visualized with ECL-plus (Amersham Biosciences) on RX-U film (Fuji, Japan).

To immunoprecipitate *Py*RhopH complexes, 50 μl of *P. yoelii* extract, 2 μl of yeast-produced recombinant Pys25 (yPys25) solution (5 mg ml^{-1}), and 2 μl (1 mg ml^{-1}) of mAb#32 were mixed and incubated at RT for 2 h with gentle rocking. Twenty microlitres of 50% Gamma Bind Plus Sepharose (Amersham Biosciences) solution were added and incubated another 1 h at RT with gentle rocking. The mixture was centrifuged at 21,600 × *g* for 5 min and supernatants were removed. The beads were washed in NETT [50 mM Tris (tris(hydroxymethyl)aminomethane)–HCl, 0.15 M NaCl, 1 mM EDTA, 0.5% Triton X-100, pH 7.5] + 1% BSA, NETT, high salt NETT (0.5 M NaCl), NETT, and 1/3 NETT (0.05 M NaCl and 0.17% Triton X-100). Supernatants were removed and bound proteins were eluted from beads by boiling at 100 °C for 3 min in 1× SDS-PAGE loading buffer and electrophoresed on a 5–20% gradient polyacrylamide gel under reducing and non-reducing conditions. As a control, mAb#16 was used to precipitate yPys25, instead of mAb#32.

2.8. Indirect immunofluorescence assay

A mouse harboring 28% GPI-deficient erythrocytes was inoculated intraperitoneally with *P. yoelii* 17X (lethal) and thin blood smears were prepared 3 days later at two time points. Blood smears were kept at −80 °C until use. Smears were fixed with 1% formaldehyde/PBS at RT for 15 min, blocked with 5% skim milk/PBS for 15 min at RT, reacted with rat anti-mouse CD24 mAb for 15 min at RT, washed with ice-cold PBS for 5 min, and reacted with FITC-conjugated goat anti-(rat IgG + IgM) mAb (BD Biosciences) for 15 min. Parasite nuclei were stained with DAPI (4′,6-diamidino-2-phenylindole; Wako) and mounted with Prolong Antifade solution (Molecular Probes, Eugene, OR). High-resolution image capture and processing were done using a fluorescence microscope (BX50; Olympus, Japan) and digital camera (IM500; Leica, Germany). Images were processed using Adobe Photoshop (Adobe Systems Inc., San Jose, CA).

2.9. Statistical analysis

The Mann–Whitney test was used to evaluate differences observed in erythrocyte binding assays. The chi-square test was used to evaluate the differences of parasite infectivity between GPI-positive and GPI-deficient erythrocytes. The Wilcoxon-Rank Sum test was used to evaluate the differences in parasite maturation.

3. Results

3.1. Flow cytometry analysis of PyRhopH complex interactions with erythrocytes

Prior to performing flow cytometry binding assays the character of parasite extracts was validated by Western blot analysis. *Py*RhopH2, *Py*RhopH3 and yPys25 [recombinant *Pys*25 protein (yPys25) was added to the parasite extracts as an internal control] could be detected by Western blot analysis using mAb#25, #32 and #16, respectively (Fig. 1A). *Py*RhopH1A and *Py*RhopH2 were co-precipitated using mAb#32, indicating that at least a partial RhopH complex is likely stable in the extract solution. *Py*RhopH1A, *Py*RhopH2 and *Py*RhopH3 were not co-precipitated with mAb#16 (Fig. 1B). Using parasite extracts the ability of *Py*RhopH complexes to bind normal, treated, and null erythrocytes was assessed by flow cytometry. Increased fluorescence intensity was detected using mAb#25 and #32 following incubation of BALB/c mouse strain erythrocytes with *P. yoelii* extract, in comparison to that without extract. No surface fluorescence increase was detected with mAb#16 recognizing control protein yPys25 (Fig. 1C). Fluorescence intensity increased in proportion to the amount of added *P. yoelii* extract, as shown in Fig. 1D.

3.2. PyRhopH complex binds specifically to mouse, but not rabbit or human erythrocytes

To determine the specificity of *Py*RhopH complex binding to erythrocytes, we examined binding using a panel of erythrocytes from other mouse strains [DBA/2 and B6], rabbit and human. The results were summarized in Table 1. Binding to DBA/2 and B6 mouse strain erythrocytes was similar to that from BALB/c mice. No binding was observed with rabbit or human erythrocytes with up to 50 μl of extract ($P < .01$). Thus *Py*RhopH complex recognized erythrocyte surface receptors from at least three different mouse strains, but not rabbit or human erythrocytes.

3.3. The erythrocyte PyRhopH complex receptor is sensitive to trypsin and chymotrypsin treatment

To characterize erythrocyte surface proteins involved in *Py*RhopH complex recognition, BALB/c and DBA/2 mouse erythrocytes were treated with trypsin or chymotrypsin. Both

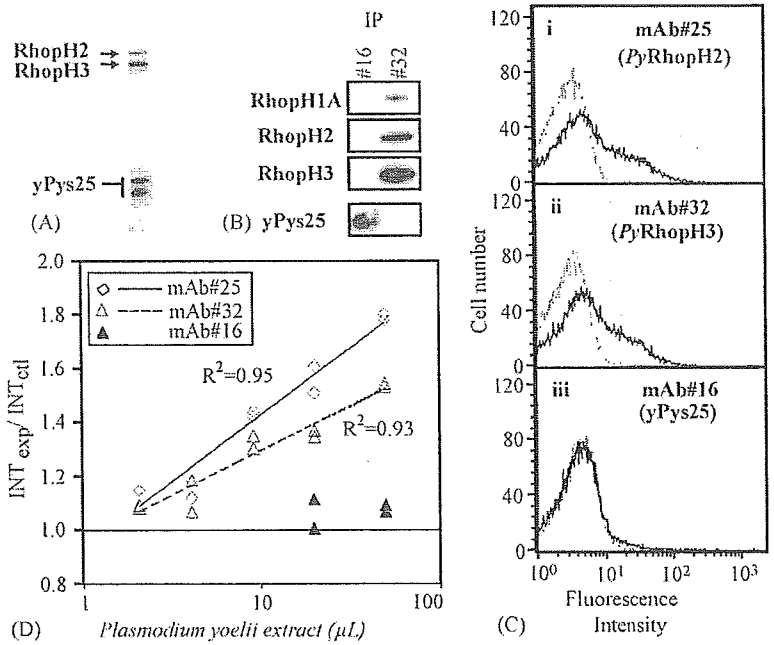

Fig. 1. *Py*RhopH complex binds mouse erythrocytes. (A) *P. yoelii* extracts were mixed with recombinant yPys25 (*Py*extract + yPys25) and subjected to Western blot analysis under non-reducing condition. The proteins were immunostained with mouse monoclonal antibodies mAb#25, #32 and #16, recognizing *Py*RhopH2, *Py*RhopH3 and yPys25, respectively. (B) Immunoprecipitation (IP) from *Py*extract + yPys25 with mAb#16 and #32 and immunostained with anti-*Py*RhopH1A mouse serum, mAb#25, #32 or #16, recognizing *Py*RhopH1A, *Py*RhopH2, *Py*RhopH3 or yPys25, respectively. The rhoptry protein complex was detected only with precipitants of mAb#32 but not mAb#16. (C) Mouse erythrocytes were incubated with *Py*extract + yPys25 (solid line) or PBS (broken line). RhopH complex binding was detected using mAb#25 or #32, followed by FITC-conjugated goat anti-(mouse IgG + IgM) antibody. A single-parameter histogram was set for FITC fluorescence of cells within the scatter gate, with a gate set on the major erythrocyte population. Fluorescence intensity increases (erythrocyte binding of *Py*RhopH complex) were observed for mouse erythrocytes with mAb#25 (i) and #32 (ii), but not with control mAb#16 that recognize yPys25 (iii). (D) The fluorescence intensity detected with mAb#25 and #32 for mouse erythrocytes increased in proportion to the amount of added *P. yoelii* extract. Representative data of multiple experiments are shown. Erythrocytes were incubated with 2, 4, 9, 20 and 50 μl of *P. yoelii* extracts and fluorescence intensity increases were measured. Geometric means were obtained for fluorescence intensities of 10,000 erythrocytes incubated with or without *P. yoelii* extract. RhopH complex binding to the erythrocyte surface was given as a value obtained by dividing the geometric mean of fluorescence intensity of the experimental sample (with extract; INT_{exp}) by that of the control sample (without extract; INT_{ctl}). Trendlines were drawn for these experiments, for which the coefficient of determination (R^2) were 0.95 (mAb#25) and 0.93 (mAb#32). Fluorescence intensities did not increase when mAb#16 was used.

Table 1
The *Py*RhopH complex binds erythrocytes of several mouse strains, but not human or rabbit erythrocytes

Erythrocyte		n[a]	INT_{exp}/INT_{ctl}[b]: median (range)	
Mouse	BALB/c	10	1.47 (1.10 – 1.80)	
	DBA/2	6	1.57 (1.38 – 1.84)	
	C57BL/6	8	1.39 (1.03 – 2.58)	
Rabbit	#1	10	0.995 (0.87 – 1.21)	
	#2	4	0.99 (0.97 – 1.04)	c
Human	#1	8	1.01 (0.95 – 1.07)	
	#2	6	0.985 (0.94 – 1.04)	c

[a]n indicates number of experiments and values were obtained from duplicated samples for each experiment. Data using mAb#25 were shown. Similar results were obtained using mAb#32 (not shown).
[b]*Py*RhopH complex binding to the erythrocyte surface were given as a value obtained by dividing the geometric mean of fluorescence intensity of the experimental samples (with extract; INT_{exp}) by that of the control samples (without extract; INT_{ctl}).
[c]Significant differences are indicated ($P<.01$).

Table 2
*Py*RhopH complex binding to mouse erythrocytes is abolished by trypsin- or chymotrypsin-treatment

Erythrocyte	INT_{exp}/INT_{ctl}[a]					
	mAb#25			mAb#32		
	BALB/c	BALB/c	DBA/2	BALB/c	BALB/c	DBA/2
Trypsin	0.97, 0.99	0.98, 1.04	0.99, 1.06[b]	0.91, 1.00	1.00, 1.00	0.97, 1.01[b]
Soy bean trypsin inhibitor	1.78, 1.91	1.24, 1.25	1.45, 1.47	1.75, 1.77	1.16, 1.19	1.25, 1.35
Chymotrypsin	0.97, 1.01	0.97, 0.97	1.00, 1.01[b]	1.04, 1.05	0.97, 0.98	0.98, 0.99[b]
TPCK	1.47, 1.52	1.09, 1.21	1.42, 1.57	1.40, 1.55	1.15, 1.27	1.33, 1.39

[a] *Py*RhopH complex binding to the erythrocyte surface were given as a value obtained by dividing the geometric mean of fluorescence intensity of the experimental samples (with extract; INT_{exp}) by that of the control samples (without extract; INT_{ctl}).
[b] Statistical differences ($P<.01$) are indicated between two groups using combined data from three experiments.

enzymes abolished *Py*RhopH complex binding ($P<.01$), indicating that a trypsin and chymotrypsin-sensitive erythrocyte receptor is likely involved in *Py*RhopH complex recognition (Table 2).

Involvement of the NANA component of erythrocyte surface proteins in *Py*RhopH complex recognition was evaluated using neuraminidase-treated erythrocytes. The efficiency of sialic acid removal was confirmed by the reduction of WGA lectin binding; specifically, to 17–24% or 20–24% of untreated erythrocytes following treatment of 100 or 200 mU ml^{-1} neuraminidase, respectively. Three independent experiments showed that *Py*RhopH binding was similar between controls and neuraminidase-treated erythrocytes, indicating that NANA was not involved in receptor recognition (not shown).

3.4. *PyRhopH complex binds to erythrocytes null for GPA and DARC*

Because the erythrocyte receptor is likely a membrane-associated protein, we were interested in determining if the known malaria parasite receptors GPA or DARC have roles as *Py*RhopH complex erythrocyte receptors. For these studies we used knockout mice disrupting these gene loci, in which the lack of the GPA or DARC expression have been confirmed [18,19]. Results of 4–5 independent experiments indicated that *Py*RhopH binding to GPA or DARC null erythrocytes was similar to binding of wild type erythrocytes, suggesting that neither GPA nor DARC are *Py*RhopH complex receptors (not shown).

3.5. *PyRhopH complex does not bind to the GPI-deficient mouse erythrocytes*

To evaluate the involvement of GPI anchors in *Py*RhopH complex binding, we used two mice harboring about 28% or 5% of GPI-deficient erythrocytes, which was determined with the surface expression of CD24. Erythrocytes from each mouse were separated into two groups based upon CD24-positivity, and *Py*RhopH complex bindings were independently measured. FL1 fluorescence intensity was increased for the GPI-positive population (Fig. 2A, upper), whereas it